Genetic screening identifies integrated stress response kinase HRI (EIF2AK1) as a negative regulator of PINK1 and mitophagy signalling

Pawan Kishor Singh[1#], Ilaria Volpi[1#], Shalini Agarwal[1], Léa P. Wilhelm[1], Giada Becchi[1], Thomas Macartney[1], Rachel Toth[1], Adrien Rousseau[1], Glenn R. Masson[2], Ian G. Ganley[1] and Miratul M. K. Muqit[1*]

[1]MRC Protein Phosphorylation and Ubiquitylation Unit, School of Life Sciences, University of Dundee, Dundee, DD1 5EH, UK

[2]Division of Cellular Medicine, School of Medicine, University of Dundee, Dundee, DD1 9SY, UK

[#]Denotes Equal contribution

*To whom correspondence should be addressed (m.muqit@dundee.ac.uk)

KEY WORDS:

PINK1, EIF2AK1, HRI, Integrated Stress Response (ISR), mitophagy

Abstract

Loss of function mutations of the PINK1 kinase cause familial early-onset Parkinson's disease. PINK1 is activated upon mitochondrial damage to phosphorylate Ubiquitin and Parkin to trigger removal of damaged mitochondria by autophagy (mitophagy). PINK1 also indirectly phosphorylates a subset of Rab GTPases including Rab8A. We have performed a siRNA screen of all human Ser/Thr kinases in HeLa cells and discovered the integrated stress response kinase EIF2AK1 (HRI) negatively regulates PINK1 following mitochondrial damage. We demonstrate that EIF2AK1 knockout cells enhance mitochondrial depolarization-induced stabilization of PINK1 and increased phosphorylation of Ubiquitin and Rab8A. We confirm our findings in multiple human cell lines including SK-OV-3, U2OS and ARPE-19 cells. Knockdown of upstream components of the recently described mitochondrial-cytosol relay pathway, OMA1 and DELE1, enhanced PINK1 stabilisation and activation similar to EIF2AK1. Using the *mito*-QC mitophagy reporter in human cells, we observe that EIF2AK1 knockdown moderately increases PINK1-dependent mitophagy. Our findings indicate that EIF2AK1 is a negative regulator of PINK1 and suggest that inhibitors of EIF2AK1 could have therapeutic benefits in Parkinson's disease and related disorders of ageing and mitophagy.

Introduction

Autosomal recessive mutations of genes encoding the mitochondrial protein kinase PTEN-induced kinase 1 (PINK1) and RING-IBR-RING (RBR) Ubiquitin E3 ligase Parkin are causal for familial early-onset Parkinson's disease (PD) [1, 2]. Upon mitochondrial depolarisation-dependent damage that can be induced in cells by chemical uncouplers (e.g. Oligomycin/Antimycin A), PINK1 undergoes stepwise activation with (1) protein stabilisation (2) recruitment to the Translocase of Outer Membrane (TOM) complex at the outer mitochondrial membrane (OMM); (3) dimerization; (4) trans-autophosphorylation of residue Serine228 (Ser228) and (5) stabilisation of loop insertion 3 within its catalytic domain that enables the recognition of substrates Ubiquitin and Parkin [3-7]. PINK1 directly phosphorylates an equivalent Serine 65 (Ser65) residue found in Ubiquitin and Parkin resulting in maximal activation of Parkin via a feed-forward mechanism triggering Ubiquitin-dependent removal of damaged mitochondria by autophagy (mitophagy) [8-10]. We have also found that PINK1 activation leads to the phosphorylation of a subset of Rab GTPases including Rab8A at a highly conserved Serine111 residue located within its RabSF3 motif [11, 12]. The mechanism of Rab protein phosphorylation by PINK1 is indirect suggesting the role of an unknown intermediate kinase [11, 12]. Furthermore, Rab8A Ser111 phosphorylation is a robust biomarker of PINK1 activation in cells and is abolished in human PINK1 knockout cells or cells expressing PD-associated mutants of PINK1 [4, 11].

To date the best characterised negative regulator of PINK1-/Parkin-induced mitophagy signalling is the deubiquitinase (DUB) USP30 discovered following an overexpression screen with a Flag-tagged human DUB cDNA library [13] and Phase I human trials of USP30 inhibitors have recently been completed successfully (Mission Therapeutics). An open question in the field is whether PINK1 is controlled by other kinase signalling pathways and networks. Herein, we have undertaken a genetic screen targeting all known human Ser/Thr kinases using endogenous PINK1-phosphorylated Rab8A at Ser111 as a readout in HeLa cells. We report the discovery of the integrated stress response kinase, EIF2AK1 (that encodes Heme Regulated Inhibitor; HRI), as a negative regulator of endogenous PINK1 stabilisation and activation and downstream mitophagy.

Results and Discussion

Genetic siRNA screen for identification of kinases that regulate endogenous PINK1-dependent Rab8A phosphorylation

To identify protein kinases that regulate endogenous PINK1-dependent Rab8A phosphorylation, we performed a siRNA screen targeting all Ser/Thr kinases in HeLa cells. We assembled and transfected a library of 428 siRNA pools (Horizon Dharmacon) targeting each kinase component for 72 hr with mitochondrial depolarisation by adding 1μM Oligomycin/10μM Antimycin A (OA) in the last 20 h of knockdown (to stabilize and activate PINK1) before cell lysis (Figure 1A). To standardize the screen, we also included untransfected cells, mock transfected

(no siRNA) and cells transfected with non-targeting (NT) siRNA as negative control and PINK1 siRNA as a positive control. As a readout of PINK1 kinase activity we monitored Ser111-phosphorylation of Rab8A deploying a previously developed phospho-specific antibody that detects endogenous PINK1-phosphorylated Rab8A by immunoblot analysis [4]. Phospho-Ser111 Rab8A and total Rab8A were quantified in parallel employing a multiplex immunoblot assay and the ratio of phospho-Ser111 Rab8A versus total Rab8A was used to calculate the degree of Rab8A phosphorylation in each cell lysate (Figure 1A). Levels of total PINK1, GAPDH and OPA1 (cleaved OPA1 is a readout of mitochondrial depolarization) were also analyzed. In addition, immunoblotting of of select kinase components of the siRNA library was performed to assess overall efficiency including BCR, TRIM28, RPS6KB2, BRD2, MAP3K7, CDC7, ROCK1, EEF2K, CAMK1D, GRK2, CSNK1A1, CSNK2A1, MAPK3, EIF2AK4, PBK/SPK, MAP3K5, MAP2K2, MAP2K6 and MAP2K7 (Supplementary Figures 1-4).

Strikingly, knock-down of the integrated stress response (ISR) kinase, EIF2AK1, enhanced phospho-Ser111 Rab8A over 1.8-fold (Figure 1B)). This was associated with an over 2-fold increase in total PINK1 levels (Figure 1C). Hits that enhanced PINK1 levels greater than 1.5-fold included SIK1 and CDK13, however, these did not significantly alter levels of phospho-Ser111 Rab8A. Conversely, we did not detect any hits that significantly reduced phospho-Ser111 Rab8A similar to PINK1 (Figure 1B). Knockdown of a number of kinases mildly reduced phospho-Ser111 Rab8A but were not significant (Supplementary Table 1).

To confirm that siRNA-mediated depletion of EIF2AK1 enhances PINK1-mediated phospho-Ser111 Rab8A, we generated a sheep polyclonal antibody against total human EIF2AK1 using recombinant full-length GST-EIF2AK1 protein expressed and purified from *E. coli* (Supplementary Figure 5A) that specifically recognizes EIF2AK1 but not the related EIF2AK4 by immunoblotting (Supplementary Figure 5B & C). Using this antibody, we were able to assess the degree of EIF2AK1 knockdown associated with PINK1 stabilisation/activation under our siRNA conditions alongside NT and PINK1 siRNA (Figure 1D). Notably we did not observe any effect of EIF2AK1 siRNA on PINK1 levels in basal/unstimulated cells indicating that EIF2AK1 regulation of PINK1 occurs only upon mitochondrial damage induced by Oligomycin/AntimycinA (OA) (Figure 1D). In addition, we observed that running lysates on 12% Tris-Glycine gels enabled visualization of an electrophoretic mobility band-shift of Rab8A that accompanied PINK1-dependent Ser111 phosphorylation and this was abolished by PINK1 siRNA knockdown and enhanced by EIF2AK1 knockdown (Figure 1D). This facile readout of phospho-Ser111 Rab8A was used in subsequent analyses. To verify the specificity of siRNA towards EIF2AK1, we performed similar experiments with independent pooled siRNA (Sigma) as well as single siRNAs (Dharmacon) for EIF2AK1 and observed that all led to enhanced PINK1 stabilisation, and PINK1-phosphorylated Rab8A as determined by Rab8A band-shift (Supplementary Figure 6A). Further we observed that EIF2AK1 siRNA knockdown increased levels of Phospho-ubiquitin consistent with increased PINK1 stabilisation and activation (Supplementary Figure 6A-C).

Previous reports in the literature have linked other ISR kinases with PD pathology such as EIF2AK3 (encoding PKR-like ER kinase; PERK) [14] and EIF2AK3 gene variants are a risk factor for the related neurodegenerative disorder, Progressive Supranuclear Palsy [15]. Moreover, ATF4 levels are increased in PINK1 and Parkin mutant Drosophila [16] however only orthologues for EIF2AK3 and EIF2AK4 (General Control Non-depressible 2; GCN2) are expressed in Drosophila and not EIF2AK1 [17]. We, therefore, compared the effect of EIF2AK1 siRNA knockdown with siRNA knockdown of the three other eIF2α kinases, EIF2AK2 (Protein Kinase R; PKR), EIF2AK3, EIF2AK4 and observed that only EIF2AK1 knockdown enhanced PINK1 stabilisation and activation (Supplementary Figure 7).

CRISPR-mediated knockout of EIF2AK1 enhances PINK1 stabilisation and activation

To further validate the role of EIF2AK1, we employed CRISPR/Cas9 gene editing technology to knock out EIF2AK1 in HeLa cells. CRISPR guides was transfected in HeLa cells and immunoblot analysis of the CRISPR EIF2AK1 knockout cellular pool lysates demonstrated increased PINK1 stabilisation and activation as judged by Phospho-ubiquitin and Rab8A Ser111 phosphorylation (band-shift) (Supplementary Figure 8). Following single-cell sorting and screening we isolated 2 independent clones from guide pair A that were confirmed by sequencing and immunoblotting to be homozygous for loss of function mutations in the EIF2AK1 gene (Supplementary Figure 9A-E). EIF2AK1 knockout cells were next treated with DMSO or OA for 12 hr to induce mitochondrial depolarization. Immunoblot analysis of whole cell lysates under basal conditions did not demonstrate any change in PINK1 levels or activity in EIF2AK1 knockout cells compared to controls consistent with the siRNA studies (Figure 2A). However, upon OA treatment, there was a robust increase in PINK1 stabilisation and activation as judged by Phospho-ubiquitin in both EIF2AK1 knockout clones compared to the wild-type control cell (Figure 2A-C). We next investigated the time course of PINK1 stabilisation, Rab8A Ser111 phosphorylation (band-shift) and Phospho-ubiquitin in EIF2AK1 knockout cells following OA treatment. We observed PINK1 proteins levels becoming stable after 3 hr of OA treatment associated with the formation of Phospho-ubiquitin and Ser111 Rab8A phosphorylation and all three readouts were enhanced in EIF2AK1 knockout cells thereby validating the siRNA studies (Figure 2D-F).

EIF2AK1 was initially implicated in a specialized role in erythrocyte (red blood cell) development whereby it is activated upon falling heme concentrations via its N-terminal heme-binding domain [18, 19]. However, it is now established that EIF2AK1 is widely expressed and responds to multiple types of signals including mitochondrial dysfunction, oxidative stress, and heat shock [20]. Mitochondrial dysfunction due to protein misfolding or mitochondrial depolarization induces up-regulation of the master transcriptional factor, ATF4 (activating transcription factor 4) and expression of ATF4-target genes [21, 22] Consistent with this we observed time-dependent up-regulation of ATF4 after 1 h treatment with OA (Figure 2D). This was abolished in EIF2AK1 knockout cells consistent with

EIF2AK1 being the primary ISR kinase activated by mitochondrial dysfunction in our system (Figure 2D).

To determine whether regulation of PINK1 stabilisation by EIF2AK1 is generalizable to other cells, we screened a panel of human cell lines including SK-OV-3 ovarian cancer cells that express PINK1 and Parkin (Wu et al., manuscript in preparation); U2OS cells that express moderate PINK1 and low levels of Parkin; and ARPE-19 retinal pigment epithelial line cells that have moderate PINK1 expression and no Parkin similar to HeLa cells (Figure 3A-E). Upon treatment of OA, we observed in all 3 cell lines, that siRNA-mediated knockdown of EIF2AK1 enhanced PINK1 stabilisation and activation as measured by Phospho-ubiquitin and Rab8A Ser111 phosphorylation (band-shift) (Figure 3A-E). Furthermore, we also observed a robust induction of ATF4 with OA treatment in all cell lines that was abolished by EIF2AK1 knockdown (Figure 3A, D, E).

OMA-1-DELE1-EIF2AK1 signalling relay negatively regulates PINK1

In previous work, two groups reported simultaneously the mechanistic details of a novel relay pathway linking mitochondrial damage with activation of the ISR and induction of ATF4 and target genes [23, 24]. They found that upon mitochondrial damage-induced activation of the mitochondrial protease OMA1, an inner mitochondrial membrane protein DELE1 is cleaved by OMA1 leading to accumulation of a shortened C-terminal fragment of DELE1 in the cytosol which binds and activates EIF2AK1. We performed siRNA studies in ARPE-19 cells in which we knocked down OMA1, DELE1 and EIF2AK1. We observed that following OA treatment, OMA1 and DELE knockdown exhibited a similar enhancement of PINK1 stabilisation and activation as EIF2AK1 consistent with the relay mechanism (Figure 4A-C). We also observed substantive reduction in ATF4 levels in DELE1 knockdown cells similar to EIF2AK1 knockdown cells but only a moderate reduction in OMA1 knockdown cells (Figure 4A, D; Supplementary Figure 10). To address whether PINK1 stabilisation by EIF2AK1 knockdown lies upstream or downstream of ATF4 reduction, we knocked down ATF4 in cells following OA treatment and observed that this was not associated with significant change in PINK1 levels and activation (Figure 4E-H). Consistent with this, when we simultaneously knocked down EIF2AK1 and ATF4 we did not see further activation compared to EIF2AK1 knockdown alone (Figure 4E-H). This indicates that ATF4 is acting downstream of PINK1 stabilisation by EIF2AK1 knockdown. Previous studies have shown that upon mitochondrial damage, PINK1 accumulates rapidly and is prevented when cells are pre-treated with the translation inhibitor, cycloheximide, suggesting that the initial mechanism for stabilization is translation and new protein synthesis [25, 26]. Consistent with this we observed that the EIF2AK1-mediated enhanced effect on PINK1 stabilisation was inhibited by cycloheximide but not the transcriptrion inhibitor, Actinomycin D (Supplementary Figure 11A-F). Activation of EIF2AK1 and the resulting phosphorylation of eIF2α reduces global protein synthesis whilst enhancing translation of ATF4 and mRNAs of key effectors of the ISR [20, 27, 28]. Mitochondrial proteins have been shown to be actively translated on the mitochondrial surface and cryo-electron tomography-visualized ribosomes have

been observed to interact with the TOM complex in basal and mitochondrial depolarization states facilitating co-translational import of select mitochondrial proteins [29, 30]. In future work it would be interesting to directly assess PINK1 translation rates on these ribosomes in EIF2AK1 knockout cells to determine if there is an increase that mediates protein stabilization. In a previous phosphoproteomic screen of mitochondrial-enriched fractions, we detected increased phosphorylation of a conserved Serine41 residue of EIF2AK1 following activation of PINK1 [11]. In future work it would be interesting to dissect the role of this site in regulation of its activation by DELE1 and downstream catalytic activity on sites of damaged mitochondria.

Role of EIF2AK1 in PINK1-dependent mitophagy

We next determined if silencing of EIF2AK1 by siRNA had an impact on PINK1-Parkin dependent mitophagy. Previous whole genome-wide siRNA and CRISPR/Cas9 screens have been undertaken for mitophagy steps including Parkin translocation to sites of damaged mitochondria or Parkin-dependent changes in mtKeima/mitophagy [31-33]. However, in these instances no components of the ISR, such as EIF2AK1, were identified. This is likely due to the high level of Parkin over-expression in these screens that is required to facilitate mitophagy detection. This may have masked the contribution of ISR kinase regulation of PINK1 due to the robust feed-forward amplification of downstream signalling conferred by Parkin. We therefore monitored mitophagy at early timepoints, in an attempt to visualise changes before the feed-forward mechanism became well established.

To monitor mitophagy, we used the previously established and well-characterised *mito*-QC assay in Parkin overexpressing ARPE19 cells [34, 35] (Figure 5 and Supplementary Figure 12A). This assay, utilising a stably expressed tandem mCherry-GFP tag attached to an OMM localisation peptide (derived from the protein FIS1), relies on a fluorescent colour change that occurs when mitochondria are delivered to lysosomes (referred to as mitolysosomes). Lysosomal acidity is sufficient to quench GFP, but not mCherry, and "red-only" mitolysosomes appear that can be easily quantified as a mitophagy readout. We observed that even under basal conditions, the silencing of EIF2AK1 moderately increased the number of mitolysosomes compared to control cells (Figure 5A and Supplementary Figure 12B). While PINK1-Parkin-dependent mitophagy was strongly induced upon mitochondrial depolarisation with Oligomycin A/Antimycin A (OA), a further mild increase of the number of mitolysosomes was also observed in EIF2AK1 silenced cells (Figure 5B and Supplementary Figure 12B). The relative increase was much smaller upon OA treatment, which is likely relective of the strong induction of the pathway due to Parkin overexpression. Overall, these results are consistent with the increased levels of phospho-ubiquitin observed upon loss of EIF2AK1 and suggest that EIF2AK1 regulates both basal and OA induced mitophagy via activation of PINK1

EIF2AK1 knockout mice have been reported to be viable and display mild alterations in erythrocytes but no gross morphological abnormalities in other tissues [19]. In future work, it would be interesting to cross EIF2AK1 knockout

mice with the mito-QC mouse reporter line [33] and determine whether EIF2AK1 loss leads to enhanced PINK1 stabilisation and stress-evoked mitophagy in the brain *in vivo*.

Conclusions

In conclusion we provide evidence that activation of EIF2AK1 acts as a negative regulator of translation of PINK1. We show by both siRNA (Figure 1 and 3) and knockout (Figure 2) that following mitochondrial depolarisation-induced stress, EIF2AK1 knockdown promotes PINK1 stabilisation and activation resulting in enhanced phosphorylation of Ubiquitin and Rab8A. We demonstrate that this is mediated indirectly by the OMA1-DELE1-EIF2AK1 relay pathway (Figure 4) and that EIF2AK1 knockdown moderately enhances PINK1-Parkin dependent mitophagy in cells (Figure 5). Our findings elaborate a model whereby the OMA1-DELE1-EIF2AK1 relay pathway is linked to PD associated with PINK1 and Parkin mutations (Figure 6). It will be interesting to investigate in the future whether these components are altered in sporadic PD where mitochondrial dysfunction is a key hallmark of disease. Furthermore, our study not only provides fundamental insights into the regulation of PINK1 but also suggests that small molecule inhibitors of EIF2AK1 may have therapeutic potential against Parkinson's and related disorders of ageing and mitophagy.

Materials And Methods

Materials

cDNA constructs for mammalian tissue culture were amplified in *Escherichia coli* DH5α and purified using a NucleoBond Xtra Midi kit (no. 740410.50; Macherey-Nagel). All DNA constructs were verified by DNA sequencing, which was performed by the Sequencing Service, School of Life Sciences, University of Dundee, using DYEnamic ET terminator chemistry (Amersham Biosciences) on Applied Biosystems automated DNA sequencers. DNA for bacterial protein expression was transformed into *E. coli* BL21 DE3 RIL (codon plus) cells (Stratagene). All cDNA plasmids, CRISPR gRNAs, antibodies and recombinant proteins generated for this study are available to request through our reagents website https://mrcppureagents.dundee.ac.uk/.

Reagents

Antimycin A (A8674), Oligomycin (75351), Cycloheximide (C7698) and Actinomycin D (A1410) were purchased from Sigma-Aldrich.

Antibodies for biochemical studies

The following primary antibodies were used: Ubiquitin phospho-Ser65 (Cell Signalling Technology (CST)), OPA1 (BD BIOSCIENCES), Rab8A (Abcam), Rab8A

phospho-Ser111 (Abcam), PINK1 (Novus), PINK1 (in-house generated by Dundee Cell Products (DCP)), GAPDH (Santa Cruz), EIF2AK2 (Abcam), EIF2AK3(Abcam), EIF2AK4(Abcam), ATF4 (Cell Signalling Technology), OMA1 (Santa Cruz), TRIM28 (Anti-KAP1) (Abcam), RPS6KB2 (Abcam), BCR (Abcam), BRD2 (Abcam), MAP3K7 (Abcam Ab109526), CDC7 (Abcam), ROCK1 (Abcam), EEF2K (Abcam), CAMK1D (Abcam), GRK2 (Abcam), CNSK2A1 (Abcam), CSNK1A1 (Abcam), GSK3B (Abcam), MAPK3 (Abcam), PBK/SPK (Abcam), MAP3K5 (Abcam), MAP2K2 (Abcam), MAP2K6 (Abcam), MAP2K7 (Abcam), HA (SIGMA or Roche). The following antibody was produced by the MRCPPU Reagents and Services at the University of Dundee in sheep: anti-EIF2AK1 (S085D).

siRNA screens and follow-up experiments

The siRNA screens were performed using a human siRNA library (Horizon Dharmacon) designed to target 428 ser/Thr kinases. The list of target siRNA pools and their oligonucleotide sequences are listed in Supplementary Table 2. 1.5 ml of Hela cells were seeded in 6-well plates at 37,000 cells/ml and transfected using 10nm of siRNA and 1.5 µl of the Lipofectamine™ RNAiMAX transfection Reagent (Thermo Fisher Scientific) per well. Cells were cultured for 52 hr after which were stimulated with Oligomycin (1 µM) and Antimycin (10 µM) (OA). After further 20 hr cells were lysates in 50 µl of Lysis buffer, centrifuged at 17,000 g for 15 min at 4°C, quantified by Coomassie (Bradford) Protein Assay Kit (WTS) and subjected to immunoblot analysis. Each siRNA screening experiment also included untreated cells, positive control PINK1 targeting siRNA, and a negative control siRNA (non-targeting siRNA, NT). The siRNA studies for further validation of EIF2AK1 with independent pooled siRNA for EIF2AK1, EIF2AK2, EIF2AK3 and EIF2AK4 as well as single siRNAs for EIF2AK1 (Dharmacon, Supplementary Table 2) were also performed as above in four different cell lines (HeLa, SKOV3, U2OS, ARPE-19). The siRNA studies for targeting OMA1 and DELE1 (Horizon Dharmacon, Supplementary Table 2) alongside EIF2AK1 were also performed in ARPE-19 cells in a similar manner.

Generation of EIF2AK1 CRISPR/Cas9 knockout cells

A full transcript map of the EIF2AK1 locus was constructed by combining data from both NCBI (NC_000007.14 (6022247..6059175, complement) and Ensembl (ENSG00000086232). Knockout (KO) guides were chosen to target as far upstream as possible within an exon common to all published and predicted variants to ensure complete disruption of all possible transcripts following CRISPR targeting. Three pairs of CRISPR/Cas9 guides were designed: A pair targeting exon 2; G1 single guide RNA targeting exon 2; and G2 single guide RNA targeting exon 2 of the EIF2AK1 gene and this would be predicted to abolish expression of full-length EIF2AK1 protein. (Supplementary Figure 9A-D). Complementary oligonucleotides were designed and annealed to generate dsDNA inserts with overhangs compatible to BbsI digested destination vectors. The sense guide insert was subsequently cloned into BbsI digested pBABED P U6 (University of Dundee DU48788) and the antisense cloned into BbsI digested pX335 (Addgene #42335), yielding clones DU69746 and DU69747 respectively.

HeLa cells were co-transfected with 1µg of each plasmid using PEI in a 10cm dish. Following 24 hr of recovery and a further 48 hr of puromycin selection (1µg/ml). The cell pool was subsequently analysed for EIF2AK1 depletion by immunoblotting then single cell sorted via FACS. Following recovery, individual clones were analysed for EIF2AK1 depletion by immunoblotting (Supplementary Figure 9E) and the promising clones A2 and A3 further verified by PCR, shotgun cloning and sequencing. Briefly, genomic DNA was isolated and a 1.8 Kb region containing exon 2 was amplified by PCR (forward primer: CACGGCATCTTTCTGCTGATCC;reverse primer: TCCAATTTTTGTATACCAGACGCTTTCC) (Supplementary Figure 9B, 9C). The resulting PCR products were subcloned into the holding vector pSC-B (StrataClone Blunt PCR Cloning Kit, Agilent Technologies) and 16 colonies (white) picked for each of the clonal lines. Plasmid DNAs were isolated and cut with EcoRI to verify insert size and 14 positive samples for each line sent for sequencing with primers M13F and M13R. Indel formation often leads to a wide range of variations between targeted alleles leading to a variety of variations between targeted alleles thus direct sequencing of amplified amplicon pools yields poor-quality data around the CRISPR target site(s). We have found in practice that analysis of >8-10 shotgun clones from a given clonal line is sufficient to verify the allelic population with precision, for hyper and hypotriploid lines more sequencing reads may be required to be confident that all alleles are accounted for. Sequencing of the A2 and A3 clones showed 3 copies of the chromosome in each case and each indel was confirmed to lead to frameshift and premature termination of EIF2AK1 further corroborating the western data (Supplementary Figure 9D) and confirming successful KO.

Cell culture and transfection

HeLa, U2OS and SK-OV-3, ARPE-19 cells were routinely cultured in standard DMEM (Dulbecco's modified Eagle's medium) supplemented with 10% (v/v) FBS, 2 mM L-glutamine, 100 U/mL penicillin and 0.1 mg/mL streptomycin. The cells were passaged by washing the cells (80-90% confluency) with PBS followed by incubation with Trypsin/EDTA. To inactivate Trypsin/EDTA (1:1) pre-warmed cell culture medium was added after 5 min and cells centrifugated at 1200 rpm for 3 min. The cell number in the suspension was counted by an automated cell counter and seeded into new culture dishes at required densities. All cells were cultured at 37°C, 5% CO_2 in a humidified incubator and routinely tested for Mycoplasma. Where indicated, cells were treated with Oligomycin (1 µM) /Antimycin A (10 µM) (OA) for mitochondrial depolarisation and 0.5 µg/ml actinomycin D, 1 µg/ml cycloheximide for the inhibition of transcription and translation respectively.

Whole-cell lysate preparation

Cells were lysed in an ice-cold lysis buffer containing 50 mM Tris-HCl, pH 7.45, 150mM NaCl, 1% (by vol) Triton X-100, 5mM $MgCl_2$, 1 mM sodium orthovanadate, 50 mM NaF, 10 mM 2-glycerophosphate, 5 mM sodium pyrophosphate, 0.5 ug/ml Microcystin LR (Enzo) and complete EDTA-free

protease inhibitor cocktail (Roche) with freshly added 1x phosphatase inhibitor cocktail (Sigma-Aldrich) and 2ul/ml Benzonase (SIGMA). Lysates were clarified by centrifugation at 17, 000g at 4°C for 15 min, and supernatants were quantified by Bradford assay (Thermo Scientific).

Immunoblotting

Samples were subjected to SDS-PAGE (Tris-glycine 12% gels) and transferred onto nitrocellulose membranes. Membranes were blocked for 1h at room temperature with 5 % non-fat milk or 5% BSA in Tris buffered saline (TBST; 50 mm Tris-HCl and 150 mm NaCl, pH 7.5) containing 0.1 % Tween-20 and incubated at 4°C overnight with the indicated antibodies, diluted in 5% bovine serum albumin (BSA) or, 5 % non-fat milk. Highly cross-absorbed H+L secondary antibodies (Life Technologies) conjugated to (IRDye® 800CW or IRDye® 680RD Infrared Dyes) were used at 1:10000 in TBST for 1h and the membrane was washed once with TBS then imaged using the OdysseyClx Western Blot imaging system.

Protein purification from E. coli

Full-length wild-type EIF2AK1 was expressed in *E. coli* as N-terminal GST fusion protein and purified as described previously for GST proteins [36]. Briefly, BL21 Codon+ transformed cells were grown at 37 °C to an OD_{600} of 0.3, then shifted to 16 °C and induced with 250 µM IPTG (isopropyl β-D-thiogalactoside) at OD_{600} of 0.5. Cells were induced with 250 µM IPTG at OD 0.6 and were further grown at 16 °C for 16 h. Cells were pelleted at 4000 r.p.m., and then lysed by sonication in lysis buffer containing 50 mM Tris-HCl (pH 7.5), 150 mM NaCl, 0.1 mM EGTA, 0.1 % (v/v) 2-mercaptoethanol, 270 mM sucrose. Lysates were clarified by centrifugation at 30 000 x g for 30 min at 4 °C followed by incubation with 1 ml of GSH Agarose resin for 1.5 h at 4 °C. The resin was washed thoroughly in wash buffer containing 50 mM Tris-HCl (pH 7.5), 200 mM NaCl, 0.5 mM TCEP, and 10% glycerol, and the protein was eluted by incubation with wash buffer containing 10 mM glutathione for 1 hr at 5° to 7°C. The eluted supernatant was dialyzed against wash buffer at 5° to 7°C overnight and concentrated, and the final sample was flash-frozen.

Mitophagy assay

ARPE-19 (ATCC, CRL-2302) cells were maintained in 1:1 DMEM:F-12 media (Thermo Scientific) supplemented with 10% (v/v) FBS, 2 mM L-glutamine, 100 U/ml penicillin and 0.1 mg/ml streptomycin. The retroviral expression vector for mito-QC was previously described (Allen et al, 2013). Vector pQCXIP HA-Parkin were generated by the DSTT, University of Dundee (DU66655). Cells stably expressing *mito*-QC mitophagy reporter system (mCherry-GFP-FIS1101–152) and HA-Parkin were seeded onto sterile glass coverslips in 12-well dishes. After treatment, coverslips were washed twice with PBS, fixed with 3.7% (w/v) formaldehyde, 200 mM HEPES pH 7.0 for 10 min and washed twice with PBS. After nuclei counterstaining with 1 µg/ml Hoechst-33258 dye, slides were washed and mounted in ProLong Gold (Invitrogen). For quantification, images were taken with Nikon Eclipse Ti widefield microscope (Plan Apo Lambda 60×

Oil Ph3 DM). All the images were processed with FIJI v1.52n software (ImageJ, NIH). Quantification of mitophagy was performed from four independent experiments counting over 60 cells per condition. Images were processed with the *mito*-QC Counter as previously described [34]. As quantitation was automated, initial blinding to sample ID was not performed.

HEK-293 transfection

HEK293 cells were transiently transfected with 5µg of each of C-terminal HA-tagged EIF2AK1 wild-type (WT) or Kinase-inactive (KI) or wild-type (WT) EIF2AK4 plasmid for 24 hr using PEI in a 10cm dish. 24 hr post-transfection, cells were lysed and immunoblotted with EIF2AK1 and HA antibodies (Supplementary Figure 5B and 5C) and membranes were analysed using the OdysseyClx Western Blot imaging system.

Acknowledgements

We thank Brett Benedetti and Shalini Padmanabhan at the Michael J Fox Foundation for helpful discussions throughout the project. We thank Anne Bertolotti at the MRC-LMB for valuable discussions on the data and critical review of the manuscript. We are grateful to the sequencing service (School of Life Sciences, University of Dundee); James Hastie for expression and generation of EIF2AK1 recombinant protein (MRC PPU); the MRC PPU tissue culture team (co-ordinated by Edwin Allen) and MRC PPU Reagents and Services antibody teams (co-ordinated by James Hastie). This work was supported by the Michael J. Fox Foundation (M.M.K.M.), a Wellcome Trust Senior Research Fellowship in Clinical Science (210753/Z/18/Z to M.M.K.M.); EMBO YIP Award (M.M.K.M.) and the Medical Research Council (MC UU 00018/8 to A.R.; MC_UU_00018/2 to I.G.G).

Conflict of Interest

M.M.K.M. is a member of the Scientific Advisory Board of Mitokinin Inc and consultant to Stealth Biotherapeutics Inc. and MSD. I.G. is consultant to Mitobridge Inc.

Figure legends

Figure 1. siRNA screens to identify kinases that regulate endogenous PINK1-dependent Rab8A phosphorylation. A: Schematic of the siRNA knockdown screens employed in this study. Hela cells seeded in 6-well plates at 0.5 * 10^6 cells/well were transfected with siRNA pools (Dharmacon) for 72 hr targeting 428 Ser/Thr Kinases with Oligomycin (1 μM)/Antimycin A (10 μM) (OA) treatment for the last 20 hr of siRNA targeting. Cells were lysed and immunoblotted for indicated antibodies and developed using the LI-COR Odyssey CLx Western Blot imaging system for quantitative analysis. **B:** Summary of data from the kinome screen. The calculated ratio of phosphorylated Rab8A/total Rab8A relative to non-targeting (NT) siRNA control, ranked from the highest increase in Rab8A phosphorylation to the strongest decrease (mean of the two replicates, SD values not shown on the chart, calculated using the Licor Image Studio software, screening blots provided in Supplementary file 1-4). **C:** As in **B**, the calculated ratio of PINK1/total GAPDH relative to non-targeting (NT) siRNA control, ranked from highest increase in PINK1 levels to the strongest decrease. **D:** Hela cells were transfected with siRNA for 72 hr with the top hit from the screen, EIF2AK1 along with the siRNA for PINK1 and non-targeting (NT) siRNA control with Oligomycin (1 μM)/Antimycin A (10 μM) (OA) treatment for the last 12 hr of siRNA targeting. Cells were then lysed and immunoblotted with pRab8A, Rab8A, PINK1, EIF2AK1, OPA1 and GAPDH antibodies and analyzed as described above.

Figure 2. CRISPR knock-out of the full-length EIF2AK1 in Hela cells enhances PINK1 stabilisation and activation. A: Wild-type Hela cells and two independent EIF2AK1 knock-out Hela cells clones A2, A3 that had all been through in parallel, single-cell sorting, and expansion were treated with Oligomycin (1 μM)/Antimycin A (10 μM) (OA) or DMSO for 12 hr.Cells were lysed and immunoblotted for pUB, PINK1, Rab8A, EIF2AK1, ATF4, OPA1, GAPDH and the immunoblots were developed using the LI-COR Odyssey CLx Western Blot imaging system. **B:** Quantification of phospho-Ubiquitin/GAPDH ratio normalised to the ratio in WT (+DMSO) samples using the Image Studio software. **C:** As in **B**, Quantification of PINK1/GAPDH ratio normalised to the ratio in WT (+DMSO) samples. **D:** EIF2AK1 knock-out clone A3 and wild-type Hela cells were further treated with OA for 0.5, 1, 3, 6, 9 and 12 hr or DMSO for 12 hr as above and analyzed for pUB, PINK1, Rab8A, EIF2AK1, ATF4, OPA1 and GAPDH. **E:** Quantification of phosphoUbiquitin/GAPDH ratio normalised to the ratio in WT (+DMSO) samples using the Image Studio software. **F:** As in **E**, Quantification of the PINK1/GAPDH ratio normalised to the ratio in WT (+DMSO) samples.

Figure 3. Validation of the EIF2AK1 mediated PINK1 stabilisation and activation across a panel of cell lines. A: ARPE-19 **D:** U2OS **and E:** SK-OV-3 cells either untreated or, treated with non-targeting control siRNA pool (NT), siRNA pool targeting PINK1, EIF2AK1, EIFF2AK2, EIF2AK3, EIF2AK4, for 72 hr were treated with Oligomycin (1 μM)/Antimycin A (10 μM) (OA) in the last 12 hr. Cells were lysed and immunoblotted for pUB, RAB8A, PINK1, EIF2AK1,

EIFF2AK2, EIF2AK3, EIF2AK4, OPA1, GAPDH and ATF4 and the immunoblots were developed using the LI-COR Odyssey CLx Western Blot imaging system. **B:** Quantification of the ARPE-19 cells for phosphoUbiquitin/GAPDH ratio normalised to the ratio in non-targeting control (+OA) samples using the Image Studio software. **C:** As in **B,** Quantification for PINK1/GAPDH ratio normalised to the ratio in non-targeting control (+OA) samples.

Figure 4. OMA1-DELE1-EIF2AK1 signaling relay negatively regulates PINK1 stabilisation and activation. A: Immunoblot of pUB, RAB8A, PINK1, EIF2AK1, EIF2AK4, OPA1, GAPDH and ATF4. ARPE-19 cells either untreated or, treated with non-targeting control siRNA pool (NT), siRNA pool targeting PINK1, OMA1, DELE1, EIF2AK1 and ATF4 for 72 hr were treated with Oligomycin (1 μM)/Antimycin A (10 μM) (OA) in the last 12 hr. **B, C, and D:** Quantification for phosphoUbiquitin/GAPDH, PINK1/GAPDH and ATF4/GAPDH ratio for figure A each normalised to the ratio in non-targeting control (+OA) samples using the Licor Image Studio software. **E:** As in A, cells either untreated or, treated with non-targeting control siRNA pool (NT), siRNA pool targeting PINK1, EIF2AK1, ATF4 or, both EIF2AK1 and ATF4 for 72 h were treated with Oligomycin (1 μM)/Antimycin A (10 μM)(OA) in the last 12 hr. **F, G, and H:** Quantification for phosphoUbiquitin/GAPDH, PINK1/GAPDH and ATF4/GAPDH ratio for figure E each normalised to the ratio in non-targeting control (+OA) samples using the Licor Image Studio software.

Figure 5. EIF2AK1 silencing slightly increases mitophagy
A, B: Representative confocal images of ARPE-19 cells that stably expressed the *mito*-QC reporter and HA-Parkin. Cells were transfected with non-targeting siRNA (NT) or siRNA targeting EIF2AK1 for 3 days prior fixation. In B, cells were treated with Oligomycin (1 μM)/Antimycin A (10 μM)(OA) for 2 hr prior to fixation. Enlarged view are shown in the lower corners. Nuclei were stained in blue (Hoechst). Scale bar: 10 μm. At right, quantification of total red-only punctate per cell (n=4 biological replicates with >67 cells per replicate.

Figure 6. Model showing integrated stress response kinase EIF2AK1 as a negative regulator of PINK1 and mitophagy signaling.
Upon mitochondrial stress OMA1 gets activated and causes cleavage of DELE1(DELE1 L) to a short form (DELE s) which accumulates in the cytosol, where it interacts with and activates EIF2AK1. Our findings suggest that activated EIF2AK1 acts as a negative regulator of PINK1-induced mitophagy signalling pathway. Besides, EIF2AK1 activation also leads to the induction of ATF4 which in turn triggers the integrated stress response (ISR).

Supplementary Figure 1-4. Primary data from siRNA Screen. A: Hela cells transfected with the indicated siRNA pools of 428 Ser/Thr Kinases (Dharmacon) for 72 hr and treated with Oligomycin (1 μM)/Antimycin A (10 μM) (OA) in the last 20 hr. Cells were lysed and immunoblotted for the indicated antibodies **Figure1.** pRab8A, Rab8A, PINK1, GAPDH, OPA1, BCR, TRIM28, RPS6KB2, BRD2 **Figure2.** pRab8A, Rab8A, PINK1, GAPDH, OPA1, MAP3K7, CDC7, ROCK1, EEF2K, CAMK1D, GRK2 **Figure3.** pRab8A, Rab8A, PINK1, GAPDH, OPA1, CSNK1A1, CSNK2A1, MAPK3, EIF2AK4, PBK/SPK, **Figure4.** pRab8A, Rab8A, PINK1, GAPDH,

OPA1, MAP3K5, MAP2K2, MAP2K6, MAP2K7. All the immunoblots were developed using the LI-COR Odyssey CLx Western Blot imaging system.

Supplementary Figure 5. Expression and purification of recombinant full-length GST-EIF2AK1 protein. A: SDS-PAGE profile of N-terminal GST-tagged EIF2AK1 protein expressed and purified from *E. coli*. **B:** HEK-293 cells transfected with C-terminal HA-tagged EIF2AK1 wild-type (WT) or Kinase-inactive (KI) and wild-type (WT) EIF2AK4 for 24 hr. Cells were lysed and immunoblotted using total human EIF2AK1 polyclonal antibody generated against full-length human N-terminal GST-tagged EIF2AK1. **C:** As in B, Immunoblotting was done using HA antibody for detection of levels of EIF2AK1 and EIF2AK4.

Supplementary Figure 6. Validation of specificity of the siRNA towards EIF2AK1. A: Hela cells were transfected with independent pooled siRNA (Sigma) as well as single siRNAs 1, 2, 3 and 4 (Dharmacon) for EIF2AK1 for 72 hr and treated with Oligomycin (1 μM)/Antimycin A (10 μM) (OA) in the last 12 hr. Cells were lysed and immunoblotted for pUB, PINK1, Rab8A, EIF2AK1, OPA1, GAPDH and immunoblots were developed using the LI-COR Odyssey CLx Western Blot imaging system. **B:** Quantification for phosphoUbiquitin/GAPDH ratio normalised to the ratio in non-targeting control using the Image Studio software. **C:** As in B**,** Quantification for PINK1/GAPDH ratio normalised to the ratio in non-targeting control (+OA) samples.

Supplementary Figure 7. Validation of the EIF2AK1 mediated PINK1 stabilisation and activation in HeLa cells. A: HeLa cells were transfected with non-targeting control siRNA pool (NT), siRNA pool targeting PINK1, EIF2AK1, EIFF2AK2, EIF2AK3, EIF2AK4, for 72 hr either untreated or, treated with Oligomycin (1 μM)/Antimycin A (10 μM) (OA) in the last 12 hr. Cells were lysed and immunoblotted for pUB, RAB8A, PINK1, EIF2AK1, EIFF2AK2, EIF2AK3, EIF2AK4, OPA1 and GAPDH and the immunoblots were developed using the LI-COR Odyssey CLx Western Blot imaging system. **B:** Quantification for phosphoUbiquitin/GAPDH ratio normalised to the ratio in non-targeting control (+OA) samples using the Image Studio software. **C:** As in B**,** Quantification for PINK1/GAPDH ratio normalised to the ratio in non-targeting control (+OA) samples. **D:** As in C**,** Quantification for ratio of phosphorylated Rab8A/total Rab8A normalised to the ratio in non-targeting control (+OA) samples.

Supplementary Figure 8. Validation of EIF2AK1 mediated PINK1 stabilisation and activation in the CRISPR knock-out pools of EIF2AK1. A: Wild-type Hela cells and Hela cells transfected with three different sets of CRISPR/Cas9 EIF2AK1 guide RNAs (A pair, G1 and G2) were treated with Antimycin A (10 μM)/ Oligomycin (1 μM) (OA) or DMSO for 12 hr. Cells were lysed and immunoblotted for pUB, PINK1, Rab8A, EIF2AK1, OPA1, GAPDH and the immunoblots were developed using the LI-COR Odyssey CLx Western Blot imaging system. **B:** Quantification for phosphoUbiquitin/GAPDH ratio normalised to the ratio in WT (+OA) samples using the Image Studio software. **C:** As in B**,** Quantification for PINK1/GAPDH ratio normalised to the ratio in WT

(+OA) samples. **D:** As in C**,** Quantification for ratio of phosphorylated Rab8A/total Rab8A normalised to the ratio in WT (+OA) samples.

Supplementary Figure 9. Generation and characterization of EIF2AK1 knockout cells. A: The sequence of EIF2AK1 in wild-type (WT) HeLa cells at exon 2 is shown and the CRISPR A pair guides used to generate EIF2AK1 Knockout (KO) is highlighted as black arrows**. B:** The flanking primer position used to confirm successful KO generation is highlighted **C:** PCR analysis of the wild-type, EIF2AK1 knockout clone A2 and A3 using exon2 flanked forward and reverse primer. PCR products were further cloned and sequenced to confirm homozygous knockout alleles. **D:** Reference exon 2 translated DNA sequence of wild-type (WT) and sequencing confirming alterations in the HeLa EIF2AK1 KO clone A2 and A3 cell lines has been highlighted. These nucleotide deletion and insertion changes in exon 2 predict a premature stop codon in all three alleles detected in EIF2AK1 KO cells. **E:** HeLa (wild-type, EIF2AK1 KO Clone A2 and A3 cell extracts were resolved by SDS–PAGE and subjected to Western blotting with EIF2AK1 polyclonal antibody.

Supplementary Figure 10. Immunoblot for validation of OMA1 knockdown by OMA1 siRNA.
ARPE-19 cells were transfected with non-targeting control siRNA pool (NT), or OMA1 for 72 hr were treated with Oligomycin (1 μM)/Antimycin A (10 μM) (OA) or DMSO in the last 12 hr. Cells were lysed and immunoblotted for pUB, PINK1, Rab8A, OMA1, ATF4, OPA1 and GAPDH and the immunoblots were developed using the LI-COR Odyssey CLx Western Blot imaging system.

Supplementary Figure 11. Effect of Cycloheximide and Actinomycin D on PINK1 stabilisation following mitochondrial depolarization in EIF2AK1 knock down cells. Hela cells were transfected with non-targeting control siRNA pool (NT), siRNA pool targeting PINK1, or, EIF2AK1, for 72 hr were either treated with **A:** Actinomycin D (Act D) (0.05 μg/ml), Oligomycin (1 μM)/Antimycin A (10 μM) (OA) or DMSO in the last 12 hr. **B, C:** Quantification for phosphoUbiquitin/GAPDH and PINK1/GAPDH ratio normalised to the ratio in non-targeting control (+OA) samples using the Licor Image Studio software. **D** As in A cells were treated with : Cycloheximide (CHX) (1 ug/ml), Oligomycin (1 μM)/Antimycin A (10 μM)(OA) or DMSO in the last 12 hr. Cells were lysed and immunoblotted and developed as indicated above. **E, F:** Quantification for phosphoUbiquitin/GAPDH and PINK1/GAPDH ratio normalised to the ratio in non-targeting control (+OA) samples using the Licor Image Studio software.

Supplementary Figure 12: Effect on EIF2AK1 silencing on PINK1-dependent mitophagy
A: Immunoblots of the indicated proteins in lysates of ARPE-19 cells transfected with non-targeting siRNA (NT) or siRNA targeting EIF2AK1 for 3 days and then treated with Oligomycin (1 μM)/Antimycin A (10 μM) (OA) for 2 hr. **B.** Violin plots of each biological replicate from Figure 5. Number of cells analyzed per independent experiment (Exp): Exp1 Basal NT: 77; EIF2AK1: 82, Induced NT: 86; EIF2AK1: 85. Exp2 Basal NT: 87; EIF2AK1: 96, Induced NT: 94; EIF2AK1: 83.

Exp3 Basal NT: 85; EIF2AK1: 76, Induced NT: 67; EIF2AK1: 82. Exp4 Basal NT: 97; EIF2AK1: 76, Induced NT: 78; EIF2AK1: 77.

References

1. Kitada, T., et al., *Mutations in the parkin gene cause autosomal recessive juvenile parkinsonism.* Nature, 1998. **392**(6676): p. 605-8.
2. Valente, E.M., et al., *Hereditary early-onset Parkinson's disease caused by mutations in PINK1.* Science, 2004. **304**(5674): p. 1158-60.
3. Gan, Z.Y., et al., *Activation mechanism of PINK1.* Nature, 2022. **602**(7896): p. 328-335.
4. Kakade, P., et al., *Mapping of a N-terminal alpha-helix domain required for human PINK1 stabilization, Serine228 autophosphorylation and activation in cells.* Open Biol, 2022. **12**(1): p. 210264.
5. Lazarou, M., et al., *Role of PINK1 binding to the TOM complex and alternate intracellular membranes in recruitment and activation of the E3 ligase Parkin.* Dev Cell, 2012. **22**(2): p. 320-33.
6. Okatsu, K., et al., *A dimeric PINK1-containing complex on depolarized mitochondria stimulates Parkin recruitment.* J Biol Chem, 2013. **288**(51): p. 36372-84.
7. Rasool, S., et al., *Mechanism of PINK1 activation by autophosphorylation and insights into assembly on the TOM complex.* Mol Cell, 2022. **82**(1): p. 44-59 e6.
8. Goodall, E.A., F. Kraus, and J.W. Harper, *Mechanisms underlying ubiquitin-driven selective mitochondrial and bacterial autophagy.* Mol Cell, 2022. **82**(8): p. 1501-1513.
9. Moehlman, A.T. and R.J. Youle, *Mitochondrial Quality Control and Restraining Innate Immunity.* Annu Rev Cell Dev Biol, 2020. **36**: p. 265-289.
10. Singh, P.K. and M.M.K. Muqit, *Parkinson's: A Disease of Aberrant Vesicle Trafficking.* Annu Rev Cell Dev Biol, 2020. **36**: p. 237-264.
11. Lai, Y.C., et al., *Phosphoproteomic screening identifies Rab GTPases as novel downstream targets of PINK1.* EMBO J, 2015. **34**(22): p. 2840-61.
12. Vieweg, S., et al., *PINK1-dependent phosphorylation of Serine111 within the SF3 motif of Rab GTPases impairs effector interactions and LRRK2-mediated phosphorylation at Threonine72.* Biochem J, 2020. **477**(9): p. 1651-1668.
13. Bingol, B., et al., *The mitochondrial deubiquitinase USP30 opposes parkin-mediated mitophagy.* Nature, 2014. **510**(7505): p. 370-5.
14. Shacham, T., C. Patel, and G.Z. Lederkremer, *PERK Pathway and Neurodegenerative Disease: To Inhibit or to Activate?* Biomolecules, 2021. **11**(3).
15. Hoglinger, G.U., et al., *Identification of common variants influencing risk of the tauopathy progressive supranuclear palsy.* Nat Genet, 2011. **43**(7): p. 699-705.
16. Celardo, I., et al., *dATF4 regulation of mitochondrial folate-mediated one-carbon metabolism is neuroprotective.* Cell Death Differ, 2017. **24**(4): p. 638-648.

17. Vasudevan, D., et al., *A protein-trap allele reveals roles for Drosophila ATF4 in photoreceptor degeneration, oogenesis and wing development.* Dis Model Mech, 2022. **15**(3).
18. Chen, J.J., *Translational control by heme-regulated eIF2alpha kinase during erythropoiesis.* Curr Opin Hematol, 2014. **21**(3): p. 172-8.
19. Han, A.P., et al., *Heme-regulated eIF2alpha kinase (HRI) is required for translational regulation and survival of erythroid precursors in iron deficiency.* EMBO J, 2001. **20**(23): p. 6909-18.
20. Costa-Mattioli, M. and P. Walter, *The integrated stress response: From mechanism to disease.* Science, 2020. **368**(6489).
21. Munch, C. and J.W. Harper, *Mitochondrial unfolded protein response controls matrix pre-RNA processing and translation.* Nature, 2016. **534**(7609): p. 710-3.
22. Quiros, P.M., et al., *Multi-omics analysis identifies ATF4 as a key regulator of the mitochondrial stress response in mammals.* J Cell Biol, 2017. **216**(7): p. 2027-2045.
23. Fessler, E., et al., *A pathway coordinated by DELE1 relays mitochondrial stress to the cytosol.* Nature, 2020. **579**(7799): p. 433-437.
24. Guo, X., et al., *Mitochondrial stress is relayed to the cytosol by an OMA1-DELE1-HRI pathway.* Nature, 2020. **579**(7799): p. 427-432.
25. Matsuda, N., et al., *PINK1 stabilized by mitochondrial depolarization recruits Parkin to damaged mitochondria and activates latent Parkin for mitophagy.* J Cell Biol, 2010. **189**(2): p. 211-21.
26. Narendra, D.P., et al., *PINK1 is selectively stabilized on impaired mitochondria to activate Parkin.* PLoS Biol, 2010. **8**(1): p. e1000298.
27. Krzyzosiak, A., A.P. Pitera, and A. Bertolotti, *An Overview of Methods for Detecting eIF2alpha Phosphorylation and the Integrated Stress Response.* Methods Mol Biol, 2022. **2428**: p. 3-18.
28. Pilla, E., K. Schneider, and A. Bertolotti, *Coping with Protein Quality Control Failure.* Annu Rev Cell Dev Biol, 2017. **33**: p. 439-465.
29. Gold, V.A., et al., *Visualization of cytosolic ribosomes on the surface of mitochondria by electron cryo-tomography.* EMBO Rep, 2017. **18**(10): p. 1786-1800.
30. Williams, C.C., C.H. Jan, and J.S. Weissman, *Targeting and plasticity of mitochondrial proteins revealed by proximity-specific ribosome profiling.* Science, 2014. **346**(6210): p. 748-51.
31. Hasson, S.A., et al., *High-content genome-wide RNAi screens identify regulators of parkin upstream of mitophagy.* Nature, 2013. **504**(7479): p. 291-5.
32. Heo, J.M., et al., *Integrated proteogenetic analysis reveals the landscape of a mitochondrial-autophagosome synapse during PARK2-dependent mitophagy.* Sci Adv, 2019. **5**(11): p. eaay4624.
33. Potting, C., et al., *Genome-wide CRISPR screen for PARKIN regulators reveals transcriptional repression as a determinant of mitophagy.* Proc Natl Acad Sci U S A, 2018. **115**(2): p. E180-E189.
34. Montava-Garriga, L., et al., *Semi-automated quantitation of mitophagy in cells and tissues.* Mech Ageing Dev, 2020. **185**: p. 111196.

35. Wilhelm, L.P., et al., *BNIP3L/NIX regulates both mitophagy and pexophagy.* EMBO J, 2022. **41**(24): p. e111115.
36. Woodroof, H.I., et al., *Discovery of catalytically active orthologues of the Parkinson's disease kinase PINK1: analysis of substrate specificity and impact of mutations.* Open Biol, 2011. **1**(3): p. 110012.

Figure 1

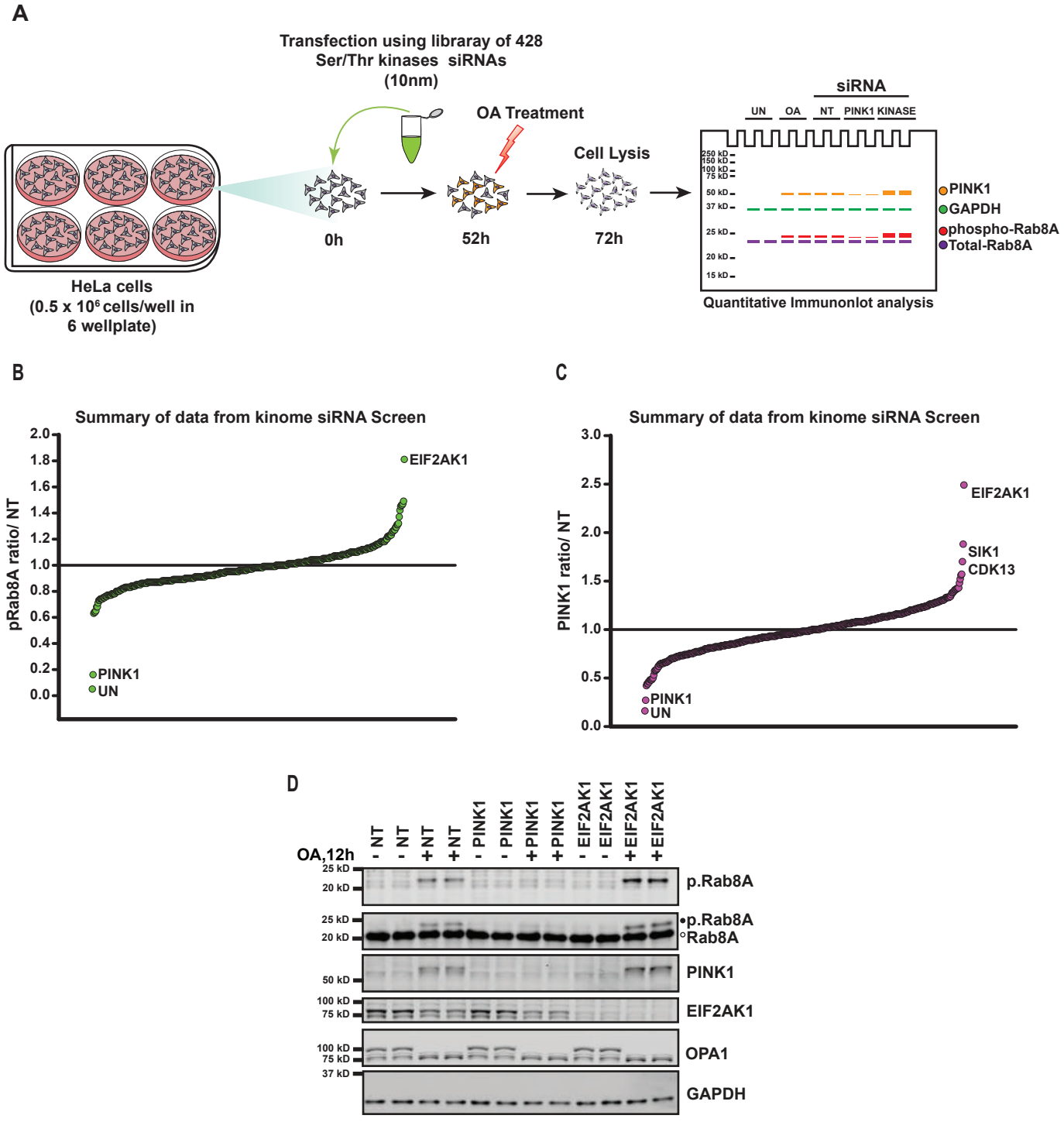

Figure 2

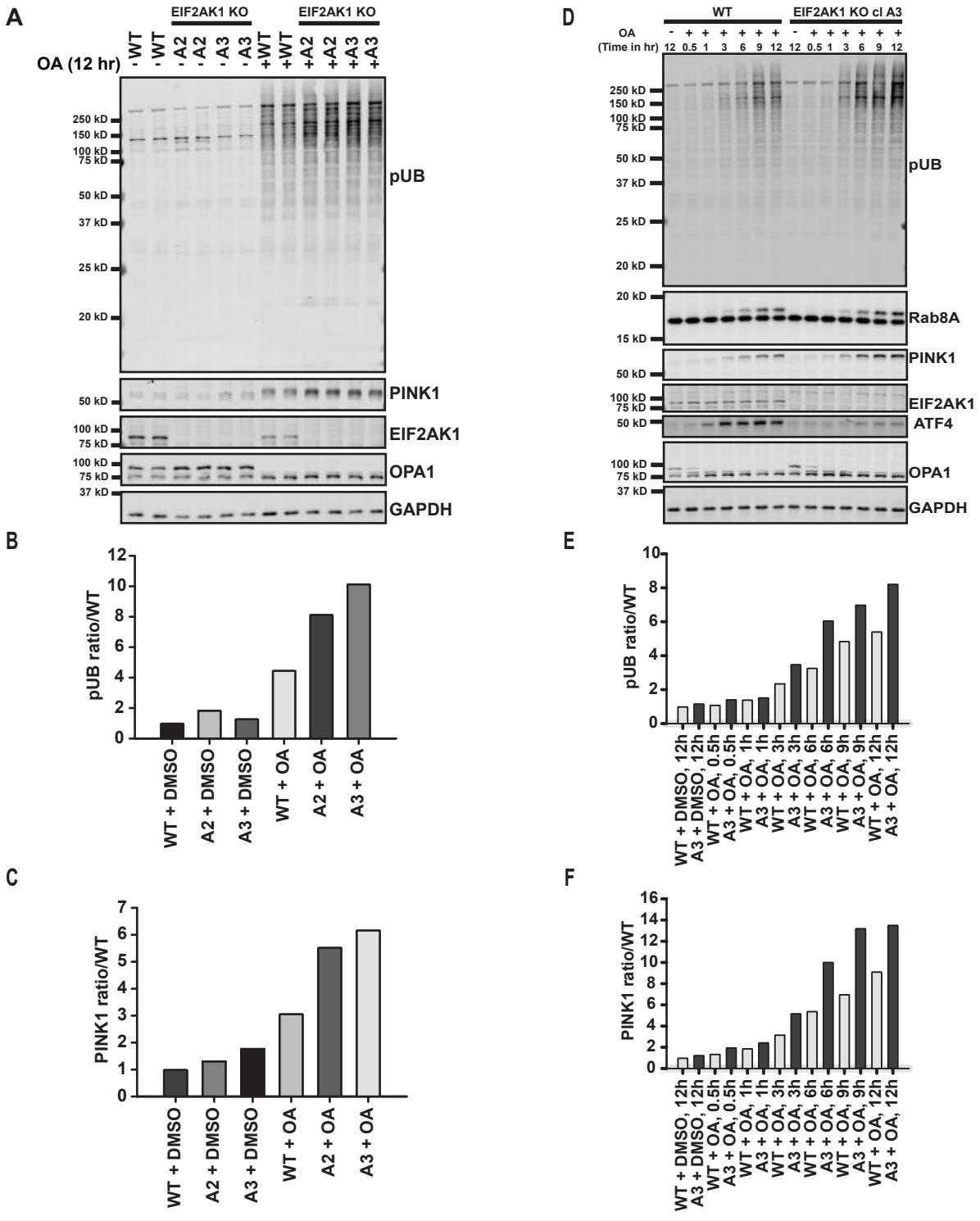

Figure 3

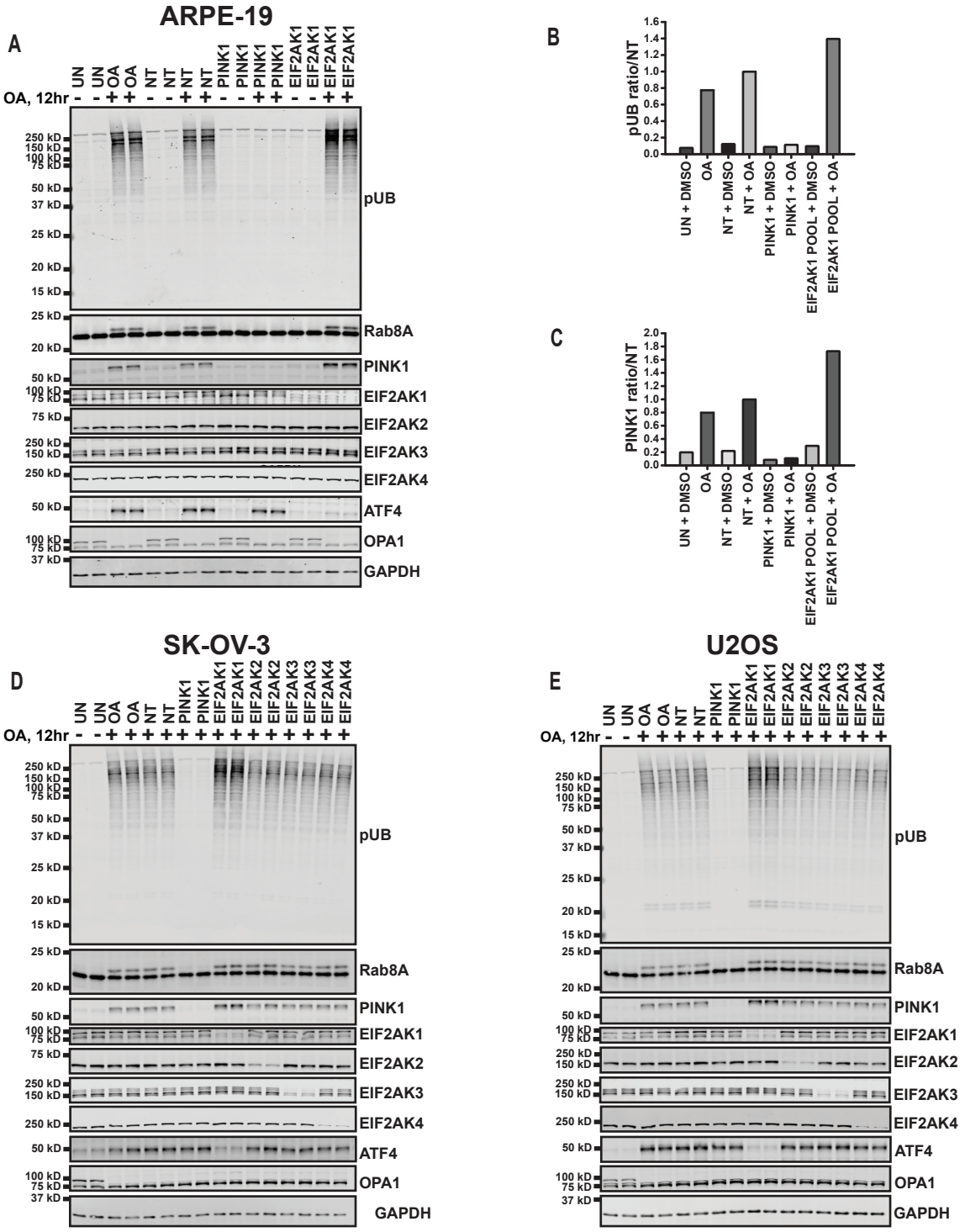

Figure 4

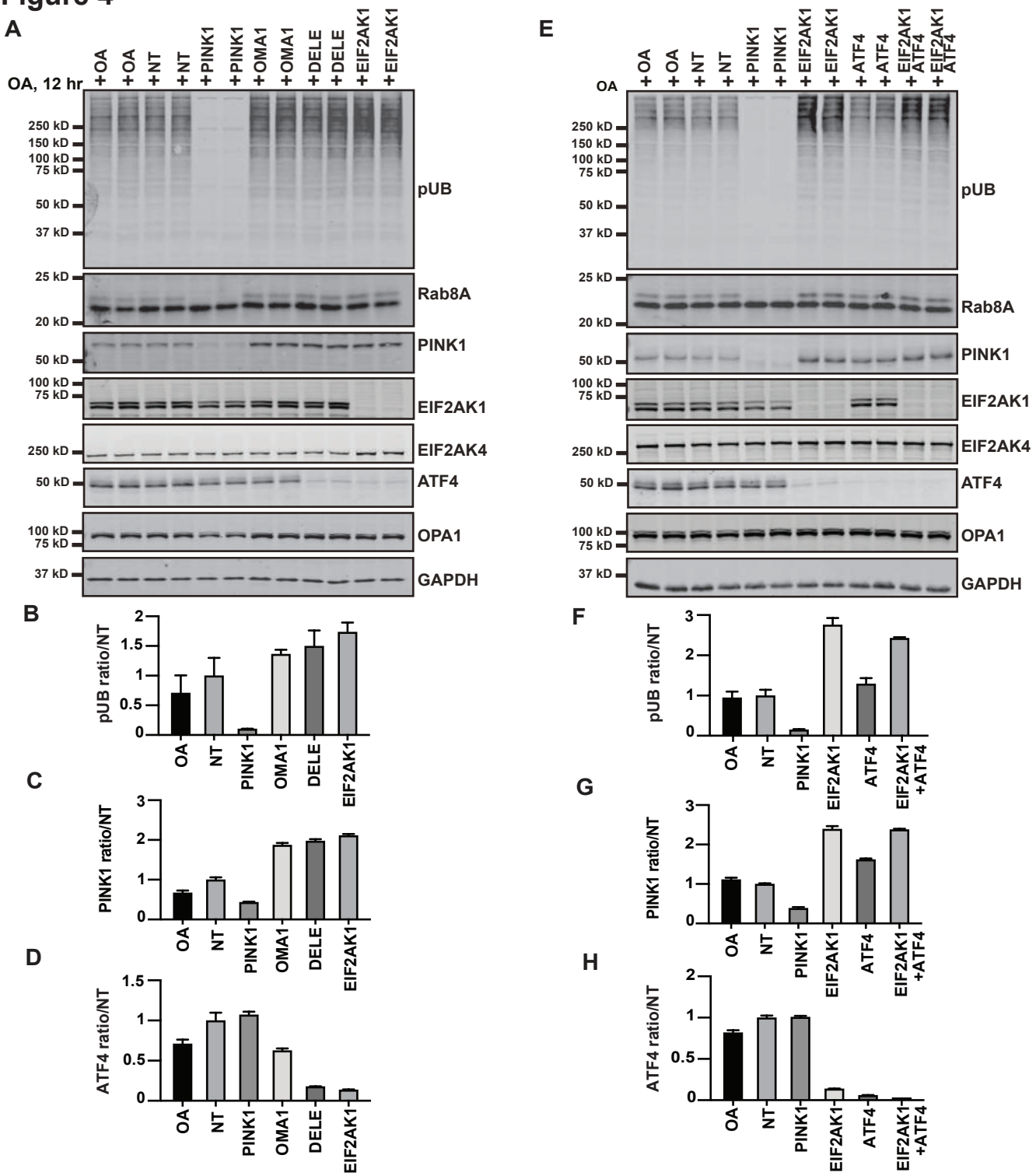

Figure 5

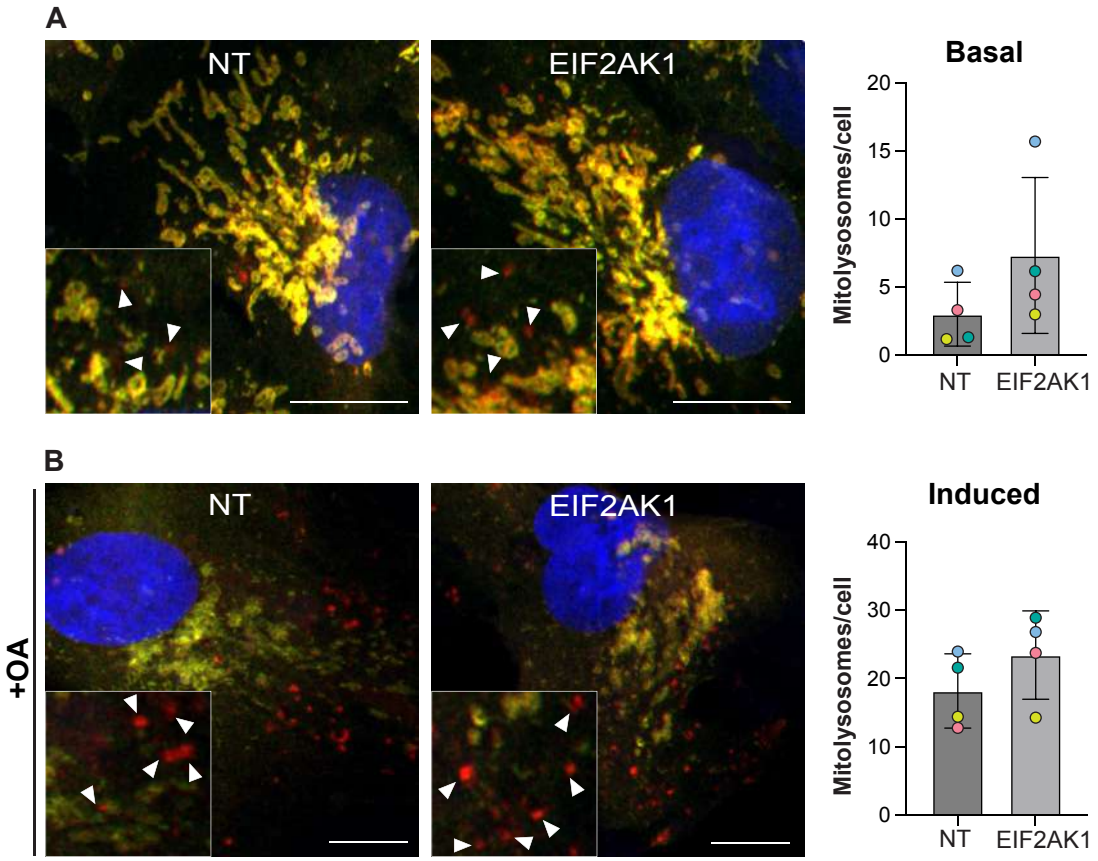

Figure 6

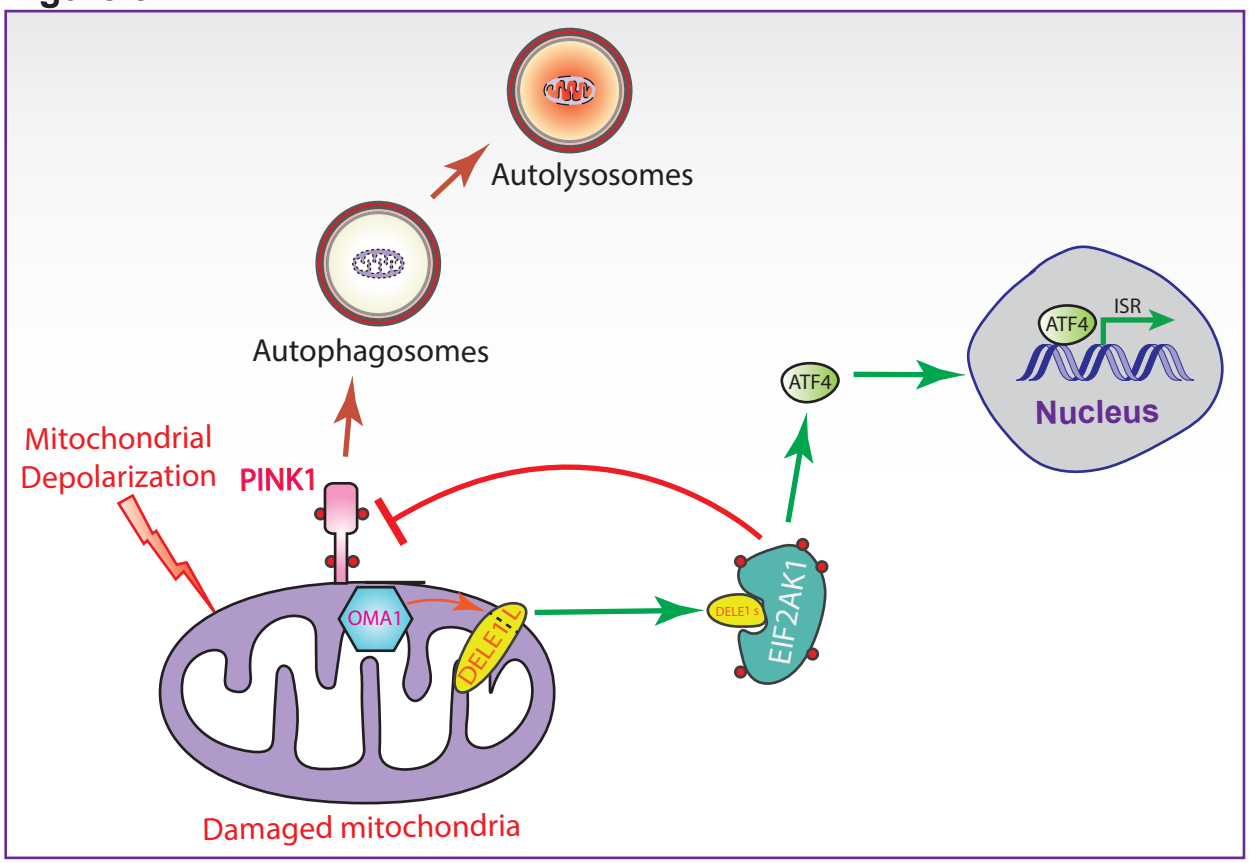

Supplementary Figure 1

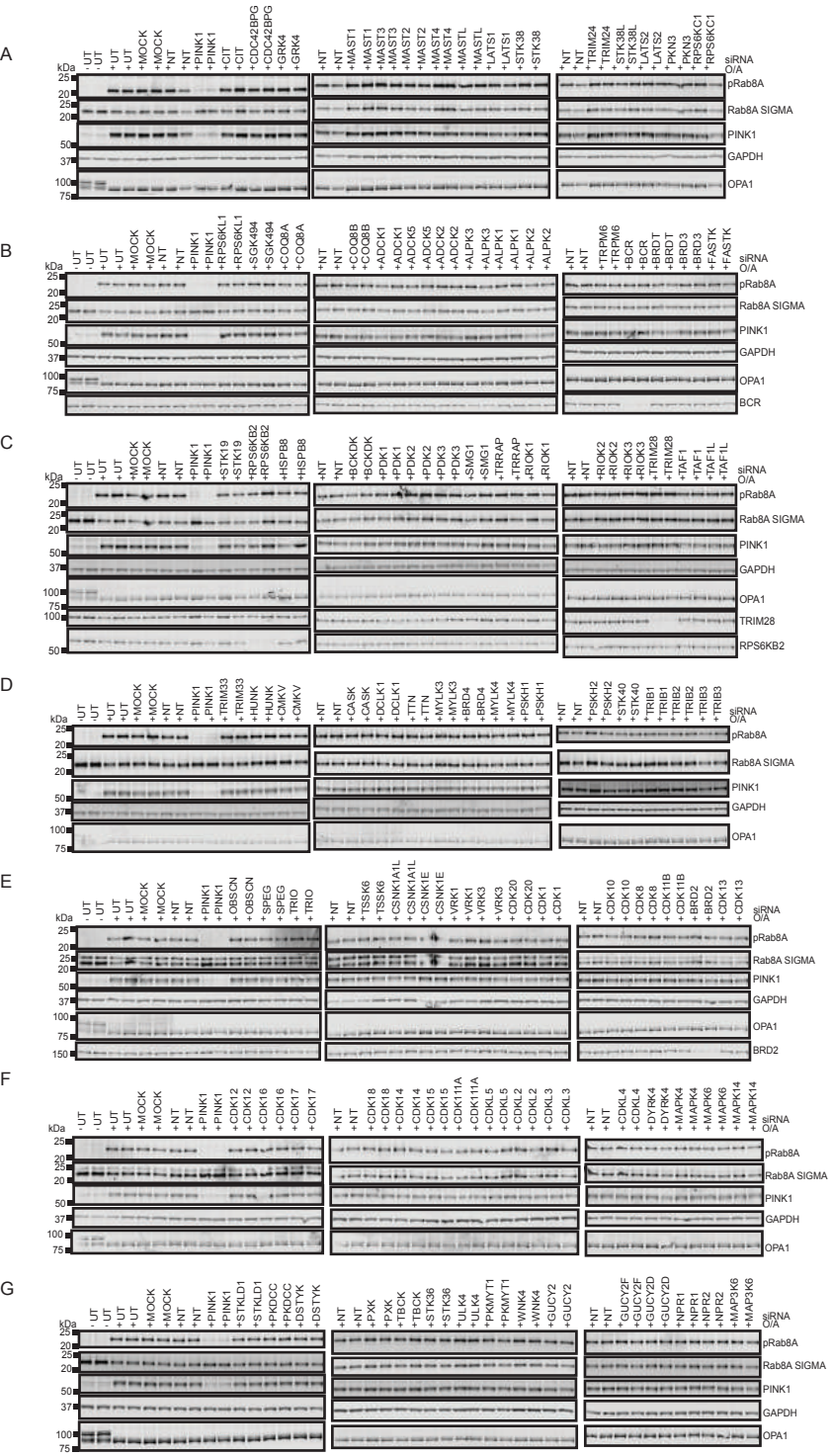

Supplementary Figure 2

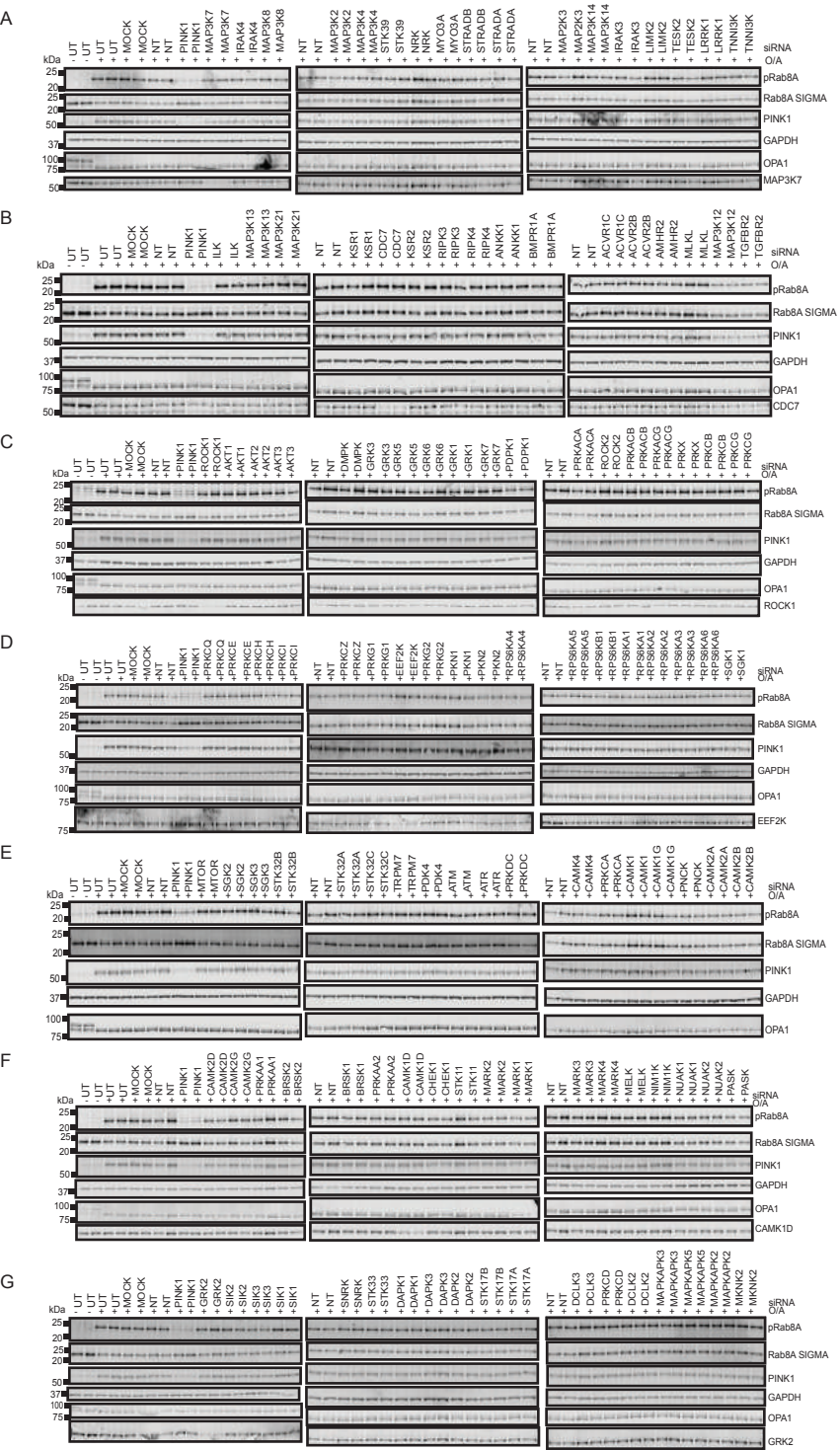

Supplementary Figure 3

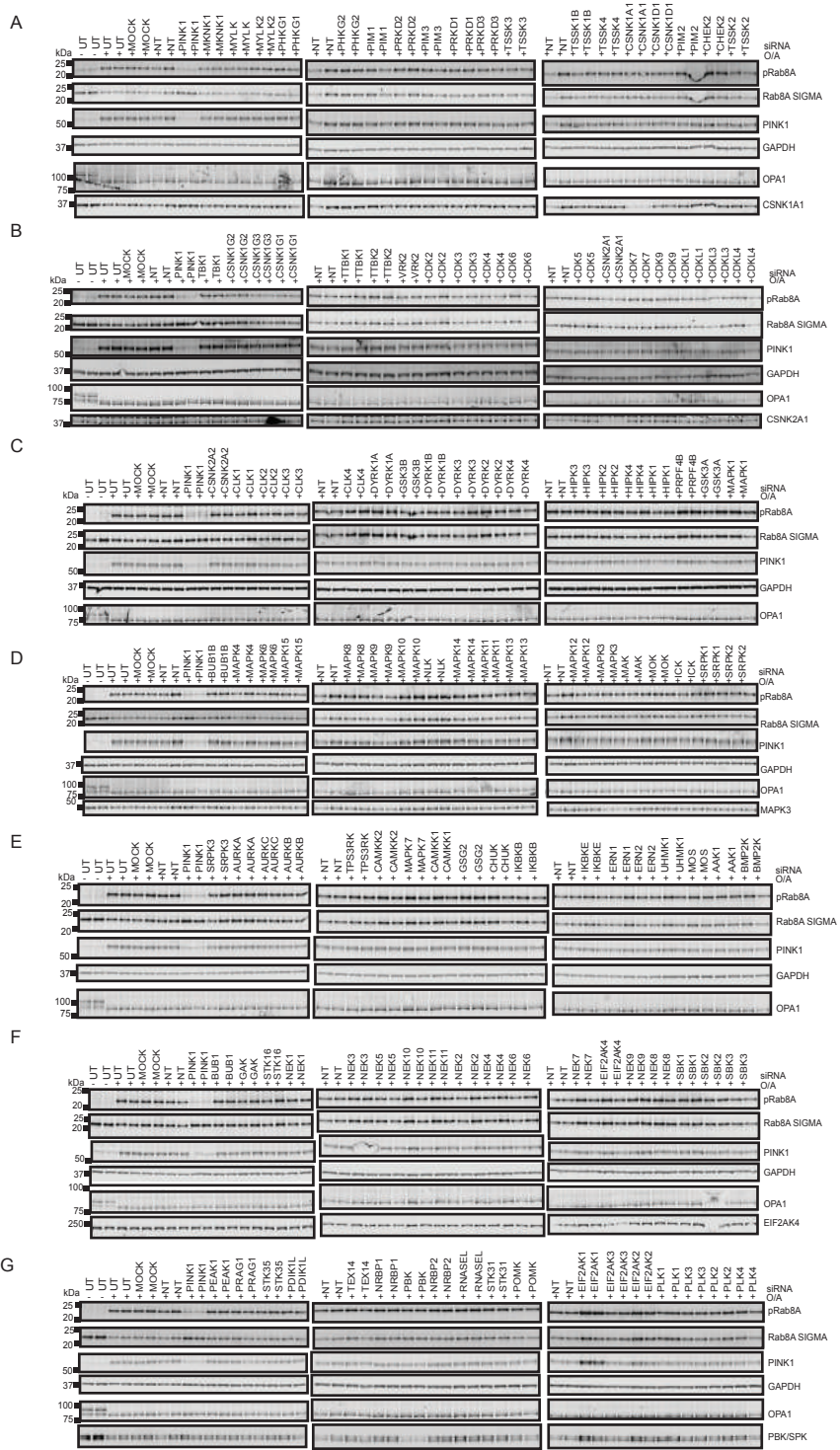

Supplementary Figure 4

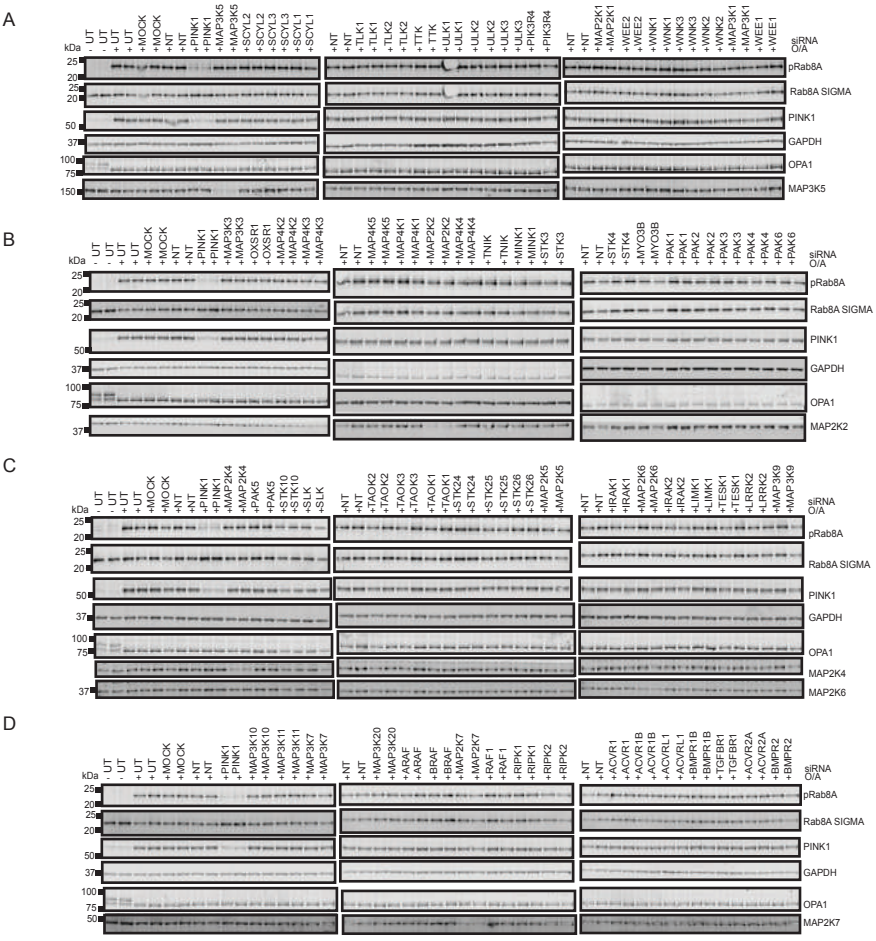

Supplementary Figure 5

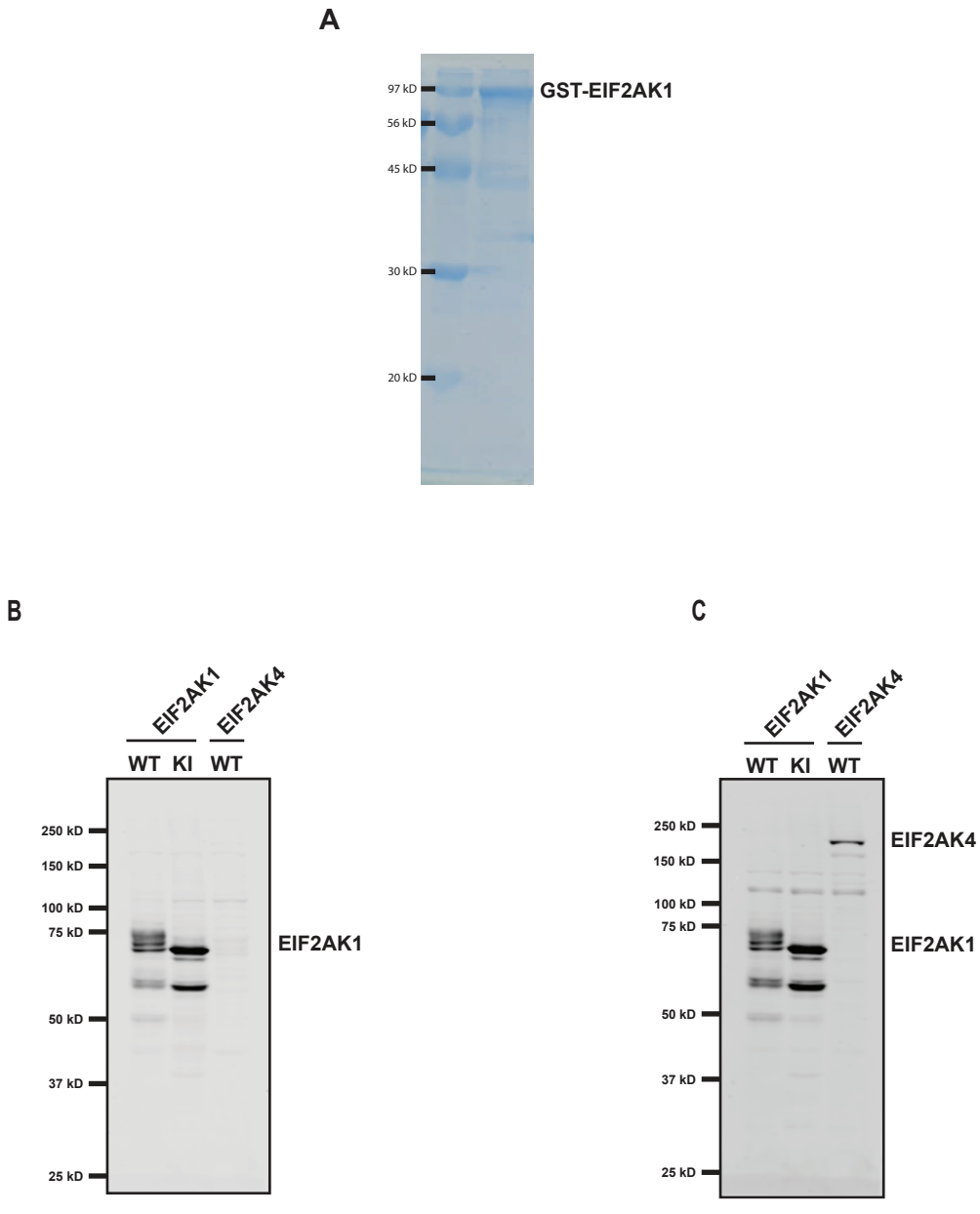

Supplementary Figure 6

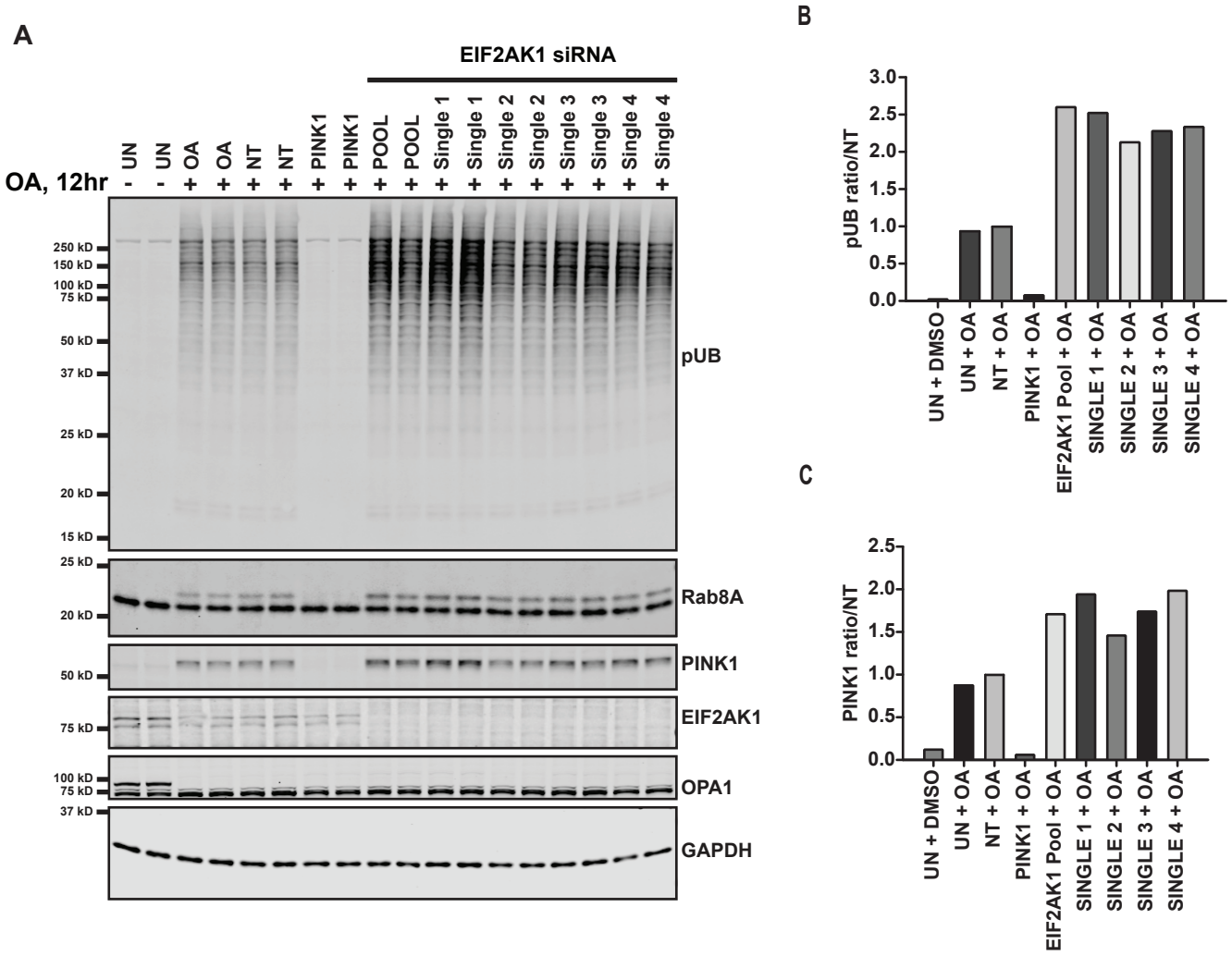

Supplementary Figure 7

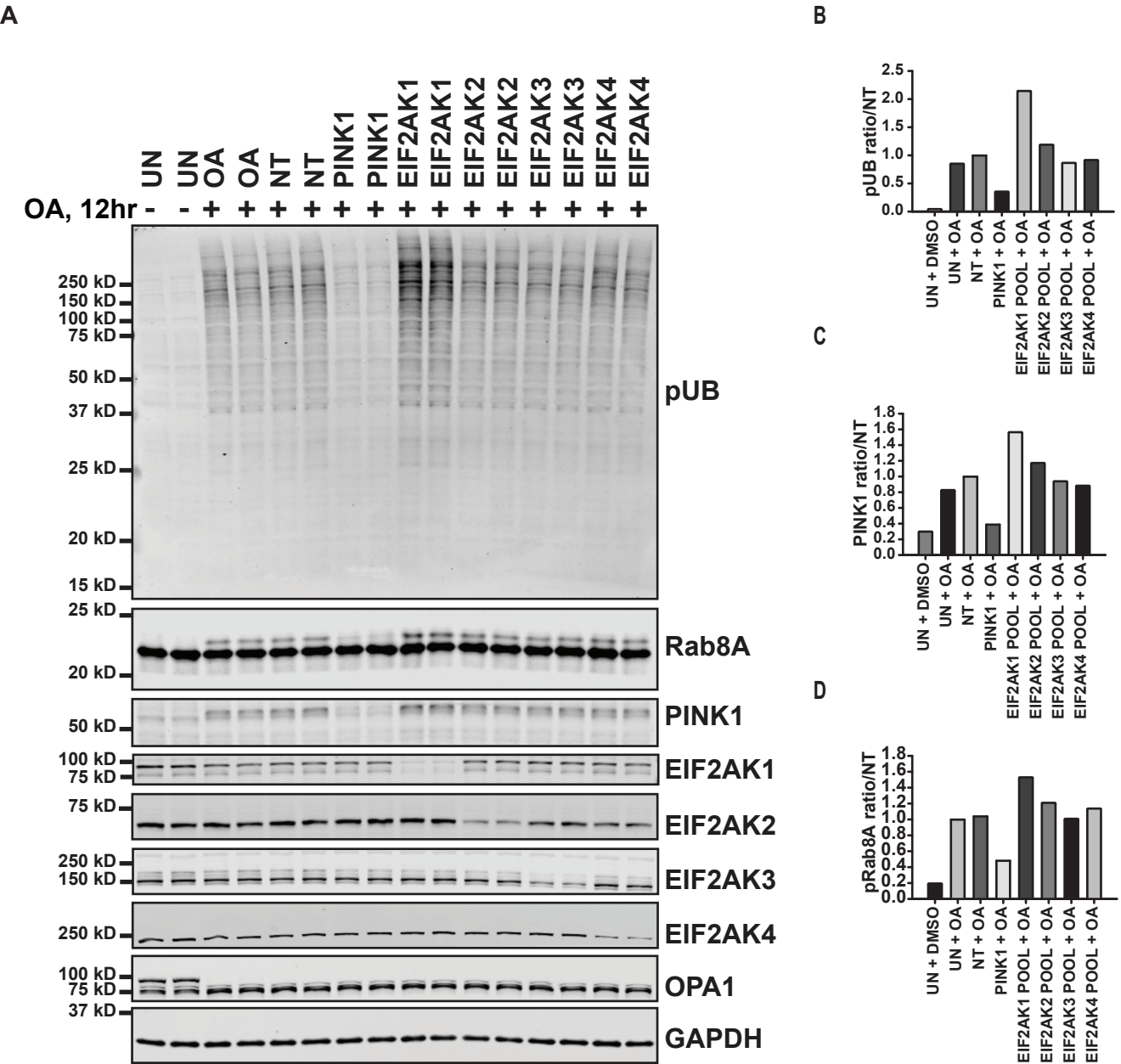

Supplementary Figure 8

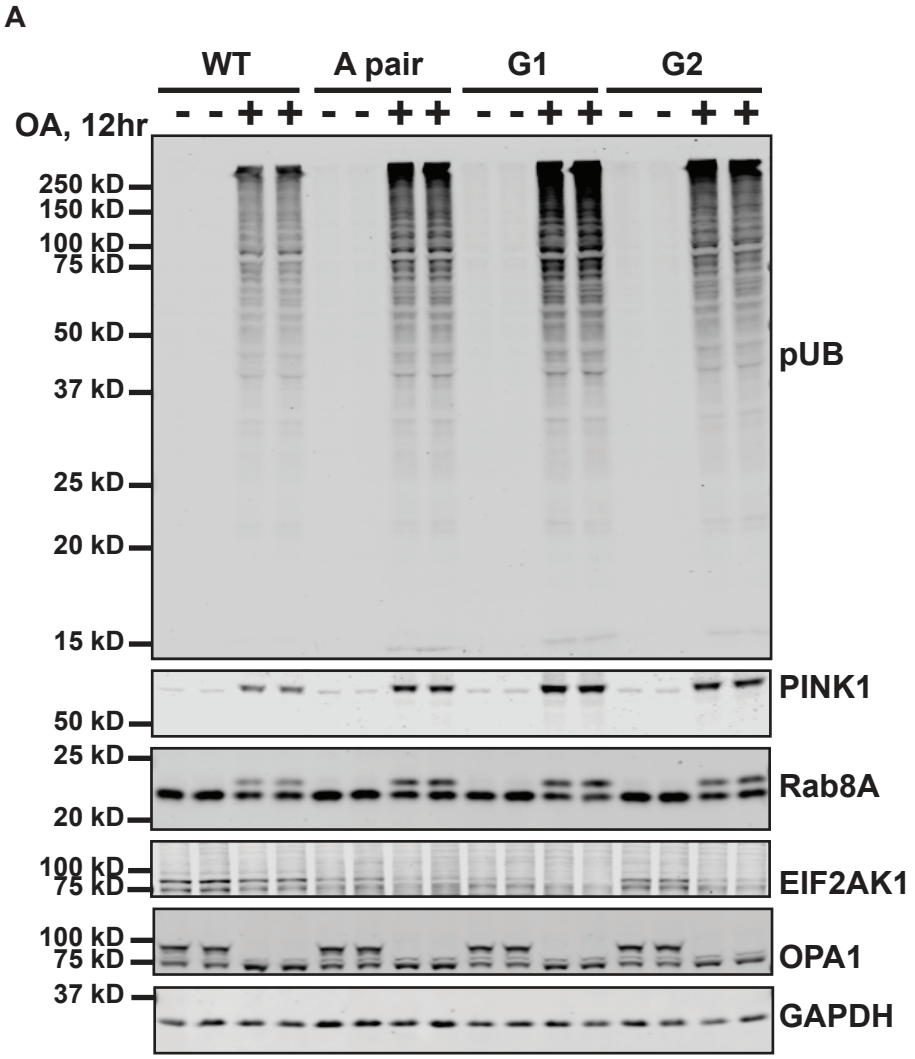

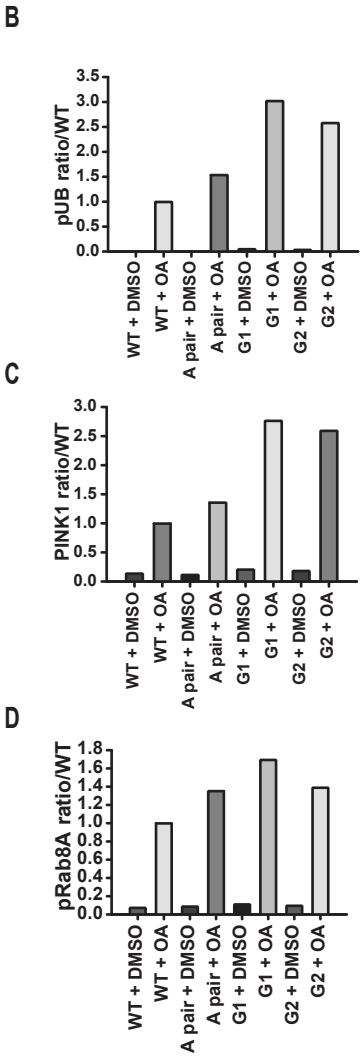

Supplementary Figure 9

A

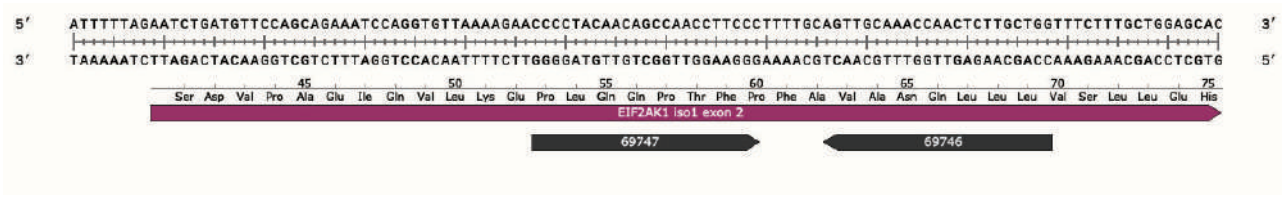

B

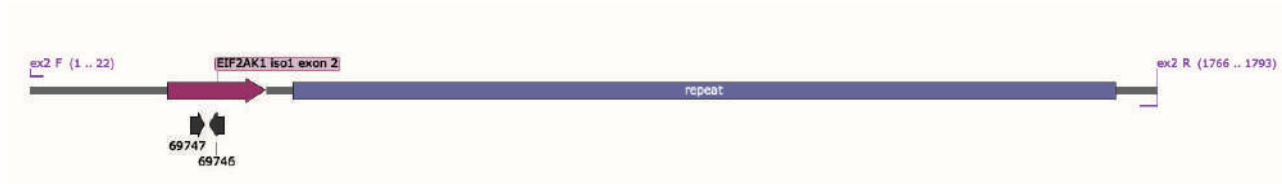

C

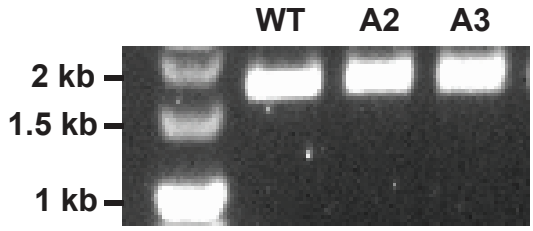

E

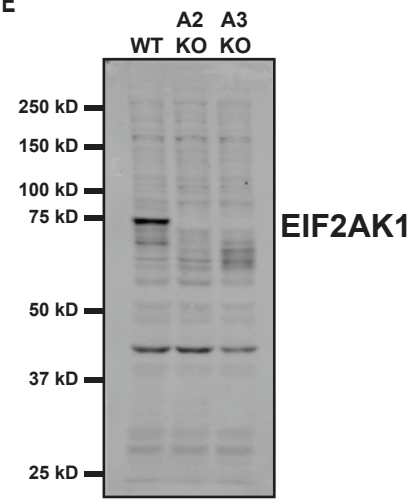

D

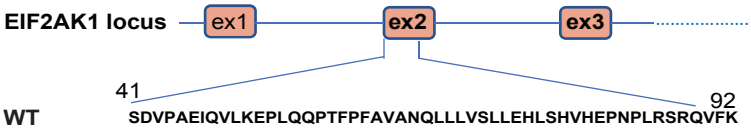

WT SDVPAEIQVLKEPLQQPTFPFAVANQLLLVSLLEHLSHVHEPNPLRSRQVFK

A2 Allele 1	SDVPAEIQVLKEPLQQQTNSCWFLCWST*	22 bp deletion
A2 Allele 2	SDVPAEIQVLKEPLQQPTFPFAGFNSQPSLLHCSCKPTLAGFFAGALEPRA*	34 bp insertion
A2 Allele 3	SDVPAEIQVLKEPLQQPTFPFAVANQQPTFPFAVANQLQLQTNSQPSLLQLQTNSCWFLCWST*	83 bp insertion
A3 Allele 1	SDVPAEIQTNLPFCSCKPTLAGFFAGALEPRA*	23 bp deletion
A3 Allele 2	SDVPAEIQVLKEPLQQPTFPFAVANQPSLLQLQTNLPFCSCKPTFPFAVANQPSLLQLQTNLPFCSCKPTLAGFFAGALEPRA*	130 bp deletion
A3 Allele 3	SDVPAEIQVLKEPLQQPTFPCWFAGFFAGALEPRA*	14 bp deletion

Supplementary Figure 10

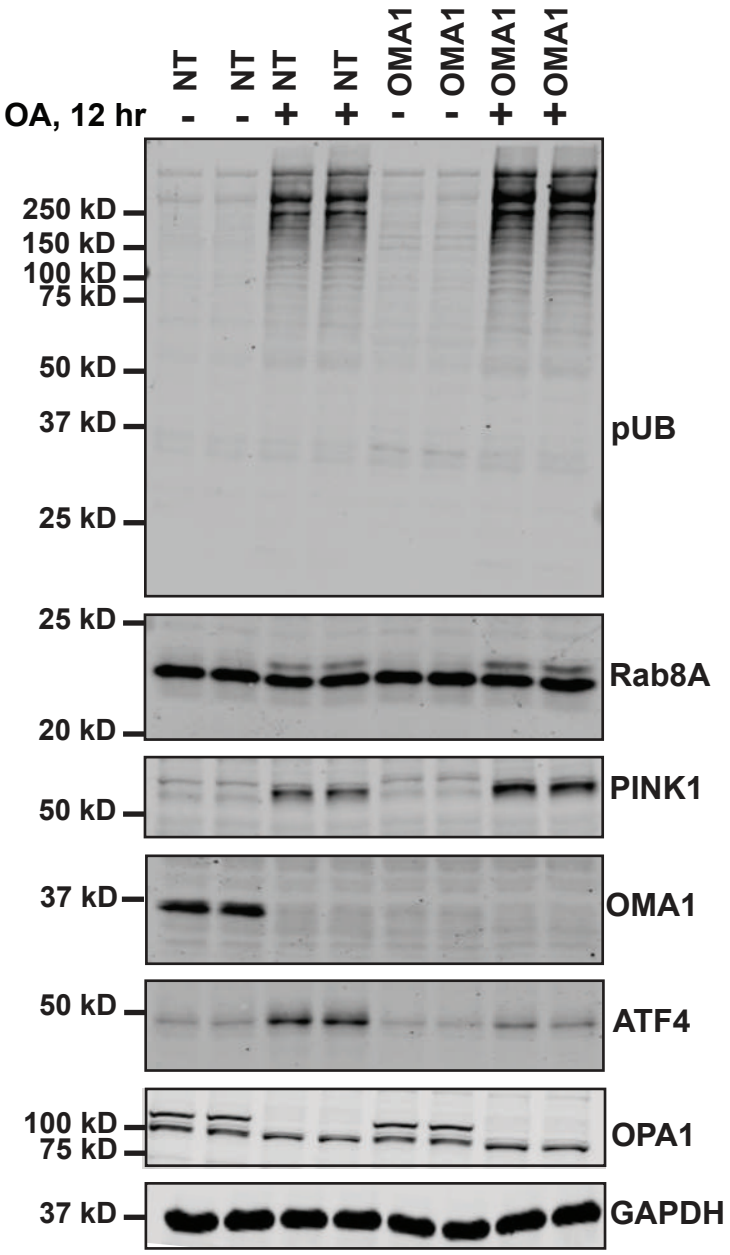

Supplementary Figure 11

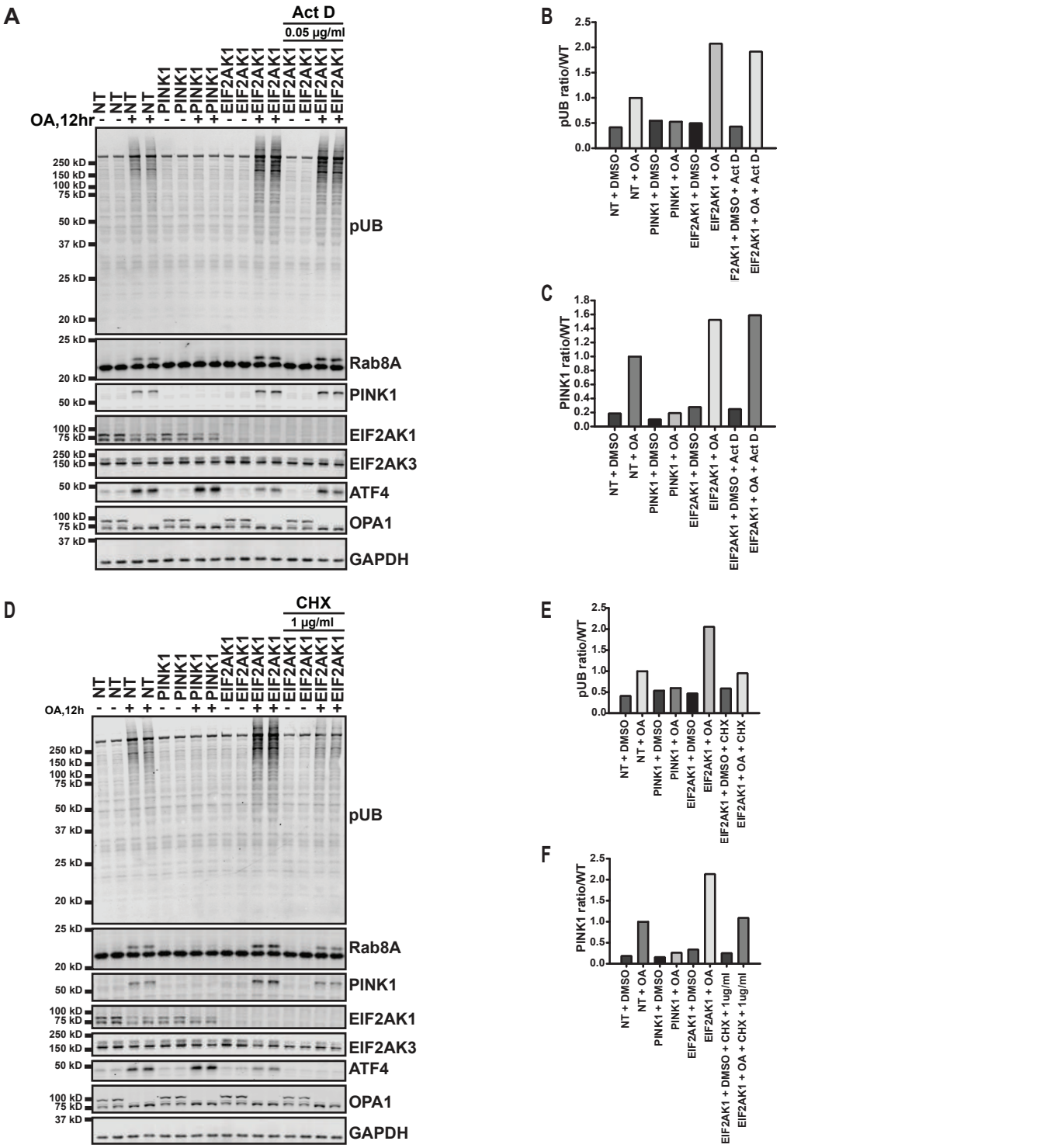

Supplementary Figure 12